Open access • Journal Article • DOI:10.1242/DEV.121.5.1283

Targeted disruption of the low-affinity leukemia inhibitory factor receptor gene causes placental, skeletal, neural and metabolic defects and results in perinatal death — Source link

Carol B. Ware, M.C. Horowitz, B.R. Renshaw, J.S. Hunt ...+6 more authors

Published on: 01 May 1995 - Development (COMPANY OF BIOLOGISTS LTD)

Topics: Leukemia inhibitory factor receptor, Leukemia inhibitory factor, Leukemia Inhibitory Factor Receptor alpha Subunit, Placentation and Glycoprotein 130

Development 121, 1283-1299 (1995)
Printed in Great Britain © The Company of Biologists Limited 1995

Targeted disruption of the low-affinity leukemia inhibitory factor receptor gene causes placental, skeletal, neural and metabolic defects and results in perinatal death

Carol B. Ware[1,†], Mark C. Horowitz[2], Blair R. Renshaw[1], Joan S. Hunt[3], Denny Liggitt[4], Simon A. Koblar[5], Brian C. Gliniak[1], Hilary J. McKenna[1], Thalia Papayannopoulou[6], Bettina Thoma[1,*], Linzhao Cheng[7,*], Peter J. Donovan[7], Jacques J. Peschon[1], Perry F. Bartlett[5], Cynthia R. Willis[1], Barbara D. Wright[1], Melissa K. Carpenter[1], Barry L. Davison[1] and David P. Gearing[1,*]

[1]Immunex, 51 University St., Seattle, WA 98101, USA
[2]Department of Orthopedics and Rehabilitation, Yale University School of Medicine, New Haven, CT 06520-8071, USA
[3]Department of Anatomy and Cell Biology, University Kansas Medical Center, 3901 Rainbow Blvd., Kansas City, KS 66160-7400, USA
[4]Department of Comparative Medicine, SB-45, University of Washington School of Medicine, Seattle, WA 98195, USA
[5]Walter and Eliza Hall Medical Research Institute, Post Office, Royal Melbourne Hospital, Parkville, Victoria 3050, Australia
[6]Division of Hematology, RG-25, University of Washington School of Medicine, Seattle, WA 98195, USA
[7]Mammalian Genetics Laboratory, ABL Basic Research Program, NCI-FCRDC, Frederick, MD 21702-1201, USA

*Present address: SyStemix, 3155 Porter Dr., Palo Alto, CA 94304, USA
†Author for correspondence

SUMMARY

The low-affinity receptor for leukemia inhibitory factor (LIFR)* interacts with gp130 to induce an intracellular signal cascade. The LIFR-gp130 heterodimer is implicated in the function of diverse systems. Normal placentation is disrupted in LIFR mutant animals, which leads to poor intrauterine nutrition but allows fetuses to continue to term. Fetal bone volume is reduced greater than three-fold and the number of osteoclasts is increased six-fold, resulting in severe osteopenia of perinatal bone. Astrocyte numbers are reduced in the spinal cord and brain stem. Late gestation fetal livers contain relatively high stores of glycogen, indicating a metabolic disorder. Hematologic and primordial germ cell compartments appear normal. Pleiotropic defects in the mutant animals preclude survival beyond the day of birth.

*Also referred to as LIF receptor β (LIFRβ; Ip, N. Y. and Yancopoulos, G. D. (1992) *Prog. Growth Factor Res.* **4**, 139-155).

Key words: osteoporosis, astrocytes, glycogen store, primordial germ cell, mouse

INTRODUCTION

Heterodimerization of low-affinity LIFR with gp130 is required for the biological activities of LIF and ciliary neurotrophic factor (CNTF) (for reviews see Gearing, 1993; Kishimoto et al., 1994). Absence of membrane-bound LIFR in mice would eliminate binding of LIF with either low or high affinity (Gearing et al., 1991, 1992; Davis et al., 1993) and eliminate signaling induced by ligand-bound CNTFRα (Ip et al., 1992; Gearing et al., 1994). Soluble LIFR serves as an antagonist to LIF signal induction (Layton et al., 1992); therefore, absence of soluble LIFR removes a naturally occurring antagonist. Additionally, human oncostatin M (OSM) can bind murine gp130 and induce a signal through murine LIFR (Gearing and Bruce, 1992; Gearing et al., 1992), although murine OSM has not yet been reported.

LIF has been implicated in murine development beginning from early embryogenesis (Conquet and Brulet, 1990; Murray et al., 1990). Some of the paradoxical data concerning the effects of LIF can be explained by the differences in developmental stage of the cells at the site of activity. LIF suppresses differentiation in embryonic stem (ES) cells (Smith et al., 1988; Williams et al., 1988) and is a survival and proliferation factor for primordial germ cells (PGC) (De Felici and Dolci, 1991; Godin et al., 1991; Matsui et al., 1991; Resnick et al., 1992). Hematopoietic effects of LIF include enhanced megakaryocyte production (Metcalf et al., 1990), platelet production after thrombocytopenia (Metcalf et al., 1992) and augmented proliferation of hematopoietic stem cells in conjunction with IL-3 (Leary et al., 1990; Verfaillie and McGlave, 1991). LIF induces differentiation of M1 myeloid leukemia cells (Tomida et al., 1984) into macrophage-like cells (Metcalf et al., 1988). Enhanced retroviral infection rate of progenitor-enriched bone marrow cultured with LIF (Fletcher et al., 1990,

1991) implicates LIF in hematopoietic progenitor cell survival. Osteoblasts, which both produce LIF and display LIFR, affect bone homeostasis (Allan et al., 1990), whereas LIF has been shown to regulate bone resorption indirectly via osteoclasts (Martin et al., 1992). Metabolic effects of LIF are suggested by LIF-induced inhibition of lipoprotein lipase production by melanoma cells (Mori et al., 1989) and by cachexia resulting from the chronic overproduction of LIF following introduction of LIF transgenes (Metcalf and Gearing, 1989a; Metcalf et al., 1990). Thus, the range of responses to LIF among individual cell types is broad and varies throughout development.

LIF also functions as a neurotrophic molecule. LIF is involved in development of fetal sensory neurons from the murine neural crest and dorsal root ganglia (DRG) (Murphy et al., 1991, 1993). After differentiation, LIF acts as a survival factor in fetal sensory neurons (Murphy et al., 1991; Hendry et al., 1992; Thaler et al., 1994) and fetal motoneurons (Martinou et al., 1992). It also supports the survival of postnatal sympathetic neurons but not until postnatal day 6 (Kotzbauer et al., 1994). Prior to this LIF has been found to trigger cell death (Kessler et al., 1993). Retrograde transport of LIF by sympathetic (Ure and Campenot, 1994) motor and sensory neurons (Hendry et al., 1992; Curtis et al., 1994) after injury suggests a role in peripheral nerve regeneration. LIF serves as a cholinergic nerve differentiation factor (Fukada, 1985; Yamamori et al., 1989; Bamber et al., 1994). This neurotransmitter switch can be compensated for by other factors in the fetus but is required during adult sympathetic neuron repair for switching to occur (Rao et al., 1993). LIF promotes the growth, maturation and survival of oligodendrocytes in vitro (Mayer et al., 1994). Pleiotropic LIF effects detected to date in the nervous system encompass mitogenicity, differentiation, cell survival and cell death, similar to the spectrum of effects of LIF seen in other physiological systems.

The gene for LIF has been disrupted by targeted mutation (Stewart et al., 1992; Escary et al., 1993). Mice homozygous for the mutation (LIF–/–) display retarded postnatal growth. Regardless of genotype, blastocysts from LIF–/– females are viable but unable to implant unless transplanted into a LIF+/+ or +/– pseudopregnant recipient, implicating a requirement for uterine endometrial LIF in the implantation process (Stewart et al., 1992). Absence of LIF reduces the number of myeloid progenitors in the spleen and impairs thymic T cell activation. However, transplantation of LIF–/– spleen or marrow cells into a wild-type host can sustain long-term host survival. This indicates the pluripotentiality of LIF–/– stem cells and the importance of LIF in the microenvironment (Escary et al., 1993).

The effects of CNTF are most apparent in the central and peripheral nervous systems. Activities attributable to CNTF are also attributable to LIF because of the shared requirement for the utilization of LIFR in combination with gp130 to promote cellular responses (for a review see Ip et al., 1992). Outside the nervous system, CNTF, like LIF, maintains ES cells in an undifferentiated state (Wolf et al., 1994; Yoshida et al., 1994), contributes to PGC survival (Cheng et al., 1994) and is implicated in the acute phase response (Akira et al., 1994; Lütticken et al., 1994). Disruption of the gene that encodes CNTF leads to an increase in atrophy of spinal motoneurons in homozygous mutant mice aged 8 weeks or older. Atrophy results in a slight reduction in muscle strength (Masu et al., 1993). The absence of the LIFR gene would be expected to cause neural defects at least as severe as those seen in adult CNTF–/– mice. Interestingly, a CNTF null mutation in humans appears to cause no neurological defects (Takahashi et al., 1994).

In this study, we show that targeted mutation of LIFR causes perinatal death. Homozygous mutant pups die during or shortly after birth if they are delivered vaginally and during the first day (P1) if delivered by Cesarean section. There are fewer LIFR–/– fetuses than expected. Placental architecture is disrupted in the LIFR–/– fetuses with a commensurate rescue response by the maternal vasculature. LIFR–/– fetuses appear grossly normal, but histological sections of late-term fetuses indicate they suffer from profound mineralized bone loss, increased liver glycogen levels and a reduction in numbers of spinal cord and brainstem astrocytes. Contrary to expectation, neither the hematopoietic system nor the primordial germ cell compartment is obviously affected. The cause of perinatal lethality is suspected to be a combination of events due to the pleiotropic nature of the defects.

MATERIALS AND METHODS

Construction of targeting vector

A murine 129/Sv genomic library (Stratagene) was screened with a radiolabeled murine LIFR cDNA probe (Gearing et al., 1991). One clone, which contained the initiator methionine, was isolated and characterized by Southern blot analysis and DNA sequencing. A 7.5 kb *Xba*I-*Sal*I fragment, from which a 120 bp fragment encompassing the start codon (ATG) had been deleted, was subcloned into a pGEM11 vector (Promega). A promoterless *lacZ* reporter gene (similar to that described by Soriano et al., 1991; Renshaw and Peschon, unpublished data) was fused to the neomycin (neo) resistance gene to produce a cassette encoding the lacZ/neo resistance fusion protein. This cassette was inserted just 3′ of the absent LIFR ATG. This vector contained 1.8 kb of LIFR homology 5′ and 5.6 kb of homology 3′ of the cassette. The lacZ/neo fusion cassette was driven by the LIFR promoter, which was left intact. *Not*I was used to linearize the vector prior to electroporation.

Electroporation and selection of ES cells

AB1 embryonic stem (ES) cells were grown on irradiated SNL feeder layers (Soriano et al., 1991) in Dulbecco's modified Eagle's medium (DMEM) supplemented with 15% fetal bovine serum (FBS, Schenk Packing, 0.22μm filtered, 3000 R γ-irradiated) and 10^{-4} M β-mercaptoethanol (ES medium) at 37°C in 5% CO_2 in air. ES cells (2×10^7 per electroporation) were electroporated with a single pulse at 200 V/960 μF using a Gene Pulser (Bio-Rad) electroporator. Cells were plated on SNL feeder layers. ES medium containing G418 (175 μg/ml effective concentration; Gibco) was added 24 hours after electroporation. Cells were cultured under selection until well-formed colonies were observed (12-14 days). Individual colonies were plated into one well of a 24-well plate seeded previously with SNL feeder cells.

Analysis of targeted clones

DNA extracted from cultured cells was subjected to PCR amplification. The primers used were 5′-TTCCCAGTCACGACGTTG-3′ (antisense 5′ lacZ primer; P2) and 5′-CCAGAACTTGTTCACTCATC-3′ (LIFR sense primer; P1) to complement sequences 5′ of the lacZ/neo insertion and sequences within the lacZ cassette (Fig. 1a,b). Only targeted clones would generate an amplification product of 1.8 kb.

Targeted clones were verified by Southern blot analysis. Genomic DNA from each targeted clone and from wild-type AB1 cells was

digested with *Eco*RI. The blots were probed with a 1.0 kb *Eco*RI-*Xba*I fragment immediately upstream of the 5′ terminus of the targeting vector. This probe hybridized with a 12.0 kb fragment in wild-type DNA. The targeting vector supplied a new *Eco*RI site downstream of the 5′ *Eco*RI site and, therefore, the probe hybridized with a 2.9 kb fragment in the targeted DNA (Fig. 1b-d).

Generation of chimeric mice

Approximately 15 ES cells with one correctly targeted LIFR allele were injected into the blastocoel of each E3.5 C57BL/6 blastocyst and transferred to uteri of E2.5 pseudopregnant Swiss Webster recipients, as described (Bradley, 1987). Transmission of the mutant allele was detected by PCR analysis after mating to 129/J females.

Genotype analysis

Heterozygosity (+/–) for LIFR was determined by the presence of the neo portion of the lacZ/neo insertion cassette. PCR amplification combined four primers: 5′-GCCCTGAATGAACTGCAGGACG-3′ (neo sense strand, P5) and 5′-CACGGGTAGCCAACGCTATGTC-3′ (neo antisense strand, P6) which amplified a 500 bp product (Fig. 1c) and primers to detect β2-microglobulin (data not shown).

DNA to determine all allelic states resulting from matings of LIFR+/– × +/– animals was prepared for genotyping by PCR analysis. The PCR reaction employed four primers: the primers described above to amplify a 500 bp product in the neo portion of the lacZ/neo cassette specific to the mutant allele and 5′-GGCCATCT-GAACAGCATCTGT-3′ (LIFR sense strand, P3) and 5′-GAAACAGGACTACTCTACGGTC-3′ (LIFR antisense strand, P4), flank the lacZ/neo insertion and amplified a 250 bp product to detect the wild-type allele (Fig. 1a,c,e). In some cases, PCR data were confirmed by Southern blot analysis as described above (Fig. 1d).

Cesarean section and fostering

Swiss Webster females as foster mothers were bred with C57BL/6 males to deliver litters on the day of Cesarean section. Pups were derived on E18.5-19.5 by Cesarean section as described (Hogan et al., 1986) and transferred to foster mothers.

MAP kinase activity

Pregnancies were disrupted on E12.5 and 15.5. Fetuses were dissociated by mincing followed by digestion with 1 mg/ml collagenase plus 1 mg/ml protease in PBS for 20-30 minutes and passaged through a 25-gauge needle. The cells from each fetus were plated into duplicate wells on 6-well plates (Costar, Cambridge, MA) at 10^6 cells per well and cultured to confluence in medium described for ES culture. Cells were pretreated for 3.5 hours at 37°C in DMEM containing 1% bovine serum albumin without FBS. Cells were stimulated with 100 ng/ml LIF, OSM or phorbol myristate acetate (PMA) for 12 minutes. Monolayers were extracted after stimulation as described (Bird et al., 1991). Cell extracts were disrupted by repeated passage through a 25-gauge needle and cleared of cellular debris by centrifugation at 10,000 ***g*** for 30 minutes.

Measurement of MAP kinase activity was performed as described (Bird et al., 1991). Briefly, 10 μl of each cell extract was added to 20 μl of kinase reaction mixture containing 20 mM Hepes, pH 7.4, 10 mM magnesium chloride, 33 μM [γ-^{32}P]ATP (2 μCi/nmol) and 1 mM substrate peptide (RRRELVEPLTPSGE) or water, for determination of peptide or nonspecific phosphorylation, respectively. Reactions were stopped after 25 minutes at 30°C by addition of formic acid. Insoluble material was removed by centrifugation for 10 minutes at 10,000 ***g*** and 30 μl of reaction mixture was spotted onto P81 phosphocellulose filters and Cerencov counted.

Delay of parturition

Progesterone (DepoProvera, Sigma M-1629) was dissolved in chloroform to 50 mg/ml and diluted in peanut oil to 2 mg/ml. Mice were injected subcutaneously with 0.1 ml of peanut oil/progesterone solution on gestational day 18.5.

Sensory neuron culture

DRG sensory neurons were isolated as described (Murphy et al., 1993). Briefly, DRG from E19.5 and P1 (E20.5) animals were dissected free of surrounding spinal tissue and chopped using 27-gauge needles. They were then incubated in Hepes-buffered Eagles medium (HEM), 0.025% trypsin, 0.001% DNase at 37°C for 30 minutes. FBS (Commonwealth Serum Laboratories, Melbourne, Australia) was added to 20% and the cells were centrifuged for 5 minutes at 300 ***g***. After resuspension in HEM containing 0.01% DNase, the cells were dispersed into single-cell suspensions by passage through 20- to 25-gauge needles. The cells were washed in HEM containing 0.01% DNase and resuspended in Monomed medium (Commonwealth Serum Laboratories) containing 10% FBS.

Wells of 24-well plates that had previously been coated with 50 μg/ml fibronectin (Boehringer-Mannheim, Indianapolis, IN) for 1 hour were seeded with 200 cells per well in Monomed medium containing 10% FBS and specified growth factors as follows: 10^3 units/ml murine LIF (Amrad, Kew, Victoria, Australia), 50 ng/ml murine 2.5S nerve growth factor (NGF) (Boehringer-Mannheim), 10 ng/ml rat CNTF (Peprotech, Rocky Hill, NJ), 10 ng/ml human OSM and 10 ng/ml murine IL-6. Five replicate wells were seeded for each animal under each culture condition. All the cells had settled in the wells after 2 hours when cultures were examined for the presence of large, phase-bright, spherical cells which were counted as neurons. Some cultures were independently stained for the presence of neurofilament to confirm neuronal identity. After determination of initial neuron numbers, the cultures were allowed to incubate at 37°C for 48 hours when the cells were fixed and stained for neurofilament. The percentage survival, where 100% is the number of neurons after 2 hours, was determined for each well. DRG from five E19.5 (2 +/+, 2 +/– and 1 –/–) and five E.20.5 (2 +/+, 2 +/– and 1 –/–) animals were assessed.

Hematopoiesis assays

Fetal liver stromal effects

Fetal liver stromas derived from LIFR+/+ and –/– E18.5 fetuses were grown to confluency under Whitlock-Witte culture conditions (Whitlock and Witte, 1982). Briefly, fetal livers were disrupted into a single cell suspension and grown in RPMI 1040 plus 5% charcoal filtered FBS (Hyclone, Logan, UT). Cultures were initiated in 6-well plates and incubated at 37°C. Non-adherent cells were continuously removed. After 2 weeks in culture, the confluent stroma layers were irradiated with 2000 rads. Freshly isolated AA4.1$^+$ LIFR+/+ or unfractionated LIFR–/– E.17.5 fetal liver cells were seeded onto the stroma at 1×10^5 nucleated cells/ml. Enrichment of AA4.1$^+$ cells, known to be enriched for fetal liver hematopoietic progenitors, was performed by cell panning as described (Lyman et al., 1993). Cells were cultured in the media described above supplemented with murine interleukin 7 (IL-7) (10 ng/ml) and murine Steel factor (SLF) (1 μg/ml). The resulting non-adherent cells were stained with fluorescein-conjugated RA3-6B2 (to identify B220$^+$ cells), GR-1 and Mac-1 antibodies. Samples were analyzed on a FACScan.

Spleen colony formation on day 14

Livers were removed from E13.5 fetuses and single-cell suspensions prepared (1 +/+, 1 +/–, 5 –/–). Individual liver suspensions were cultured overnight in DMEM supplemented with 10% FBS (Intergen, Purchase, NY), penicillin/streptomycin/ glutamine, non-essential amino acids, 10 ng/ml human IL-3 and 100 ng/ml murine SLF. Hematopoietic progenitor cell growth frequency was determined by the spleen colony forming assay (CFU-s14) (Till and McCulloch, 1961). Briefly, 6- to 9-week-old adult C57BL/6 × 129 hybrid mice were exposed to 1000 rad of gamma irradiation from a ^{137}Cs source (Mark 1 irradiator; Shepard and Associates, Glendale, CA) at a dose rate of 245 rads per

minute. Each mouse was injected intravenously with 7×10^4 fetal liver cells (6-10 mice per fetal liver). The recipient mice were killed after 14 days, the spleens were removed into Teleyesniczki's solution and macroscopic spleen colonies (CFU-s14) were counted.

Erythroid burst forming units

After overnight culture as described above for CFU-s14, fetal liver cells were plated in 0.5 ml methylcellulose (Stem Cell Technologies, Vancouver, BC) supplemented with 10 ng/ml IL-3 and 2 units/ml erythropoietin at 4×10^4 cells/ml. Erythroid colonies (BFU-e) were counted on day 7 of culture.

Erythroid colony morphology

Cells from individual E15.5 fetal livers (2 +/+, 2 +/–, 7 –/–) were plated in quadruplicate at 10^5 cells per 35 mm plate in Iscove's Modified Dulbecco's Medium (IMDM) containing 1.2% methylcellulose (Fisher), 30% FBS (Summit Biotechnology, Fort Collins, CO), 1% BSA, 10^{-4} M β-mercaptoethanol, 5 units/ml erythropoietin, 10% of 5-fold concentrated WEHI 3 conditioned medium, 5% pokeweed mitogen spleen cell conditioned medium and 50 ng/ml recombinant rat SCF. After 8 days in culture at 37°C colony formation was assessed with the aid of a dissecting microscope. Colony size was the primary criterion for distinguishing colony morphology. CFU-e were the smallest colonies made up entirely of red cells. Mature BFU-e were medium sized colonies, also made up exclusively of hemoglobin-bearing erythrocytes. Primitive BFU-e were the largest colonies and comprised a mixture of red with colorless cells.

Histological examination

E10.5-18.5 fetuses and/or maternal-fetal interfaces (placental attachment to decidua and metrial gland) were fixed in 10% neutral buffered formalin or 4% paraformaldehyde for paraffin sectioning. Fetal paraffin blocks were cut in 4 or 7 μm sections and deparaffinized and hydrated to water prior to staining. Some fetal sections were stained with hematoxylin and eosin or periodic acid-Schiff (PAS). For PAS, slides were placed in 0.5% periodic acid (Sigma) for 10 minutes. They were rinsed in water and placed in Schiff reagent (Sigma) for 30 minutes, washed and counterstained with Gill 3 hematoxylin (Sigma). Slides treated with diastase to digest sugars were compared with untreated slides to control for specificity of PAS staining.

Paraffin embedded fetal sections described above were visualized immunohistochemically with antibodies to glial fibrillary acidic protein (GFAP) using a Ventana ES Immunostaining system (Ventana, Tucson, AZ). A polyclonal rabbit GFAP antibody (BioGenex, San Ramon, CA) was used. Following exposure to biotinylated goat anti-rabbit IgG (Vector, Burlingame, CA) slides were visualized using a DAB detection kit (Ventana, 250.001). Controls were either not exposed to the anti-GFAP antibody or were incubated with anti-human IgG1 prior to visualization using biotinylated secondary antibody as described above.

Sensory neuron cultures from DRG were fixed in methanol at –20°C for 30 minutes, washed in PBS three times, incubated successively in HEM containing 2% FBS for one hour and exposed to an antibody for p150 neurofilament (Chemicon, Temecula, CA) diluted in HEM plus 1% FBS (Murphy et al., 1991). The cultures were washed three times in PBS and incubated for 45 minutes in a biotinylated anti-rabbit IgG (Vector, Burlingame, CA) diluted 1:200 in HEM containing 2% FBS. They were washed three times in PBS and incubated for 45 minutes with an avidin-biotin-peroxidase complex (Vector) followed by a 6- to 10-minute incubation in diaminobenzidine tetrahydrochloride (1 mg/ml) and hydrogen peroxidase (0.3% of a 30% solution). The cultures were then washed three times in PBS and stored as monolayers in PBS containing 0.1% sodium azide until assessed by microscopic examination.

Lower bodies of fetuses to be used for primordial germ cell PGC analysis were fixed in 4% paraformaldehyde for 2 hours (E10.5-11.5)

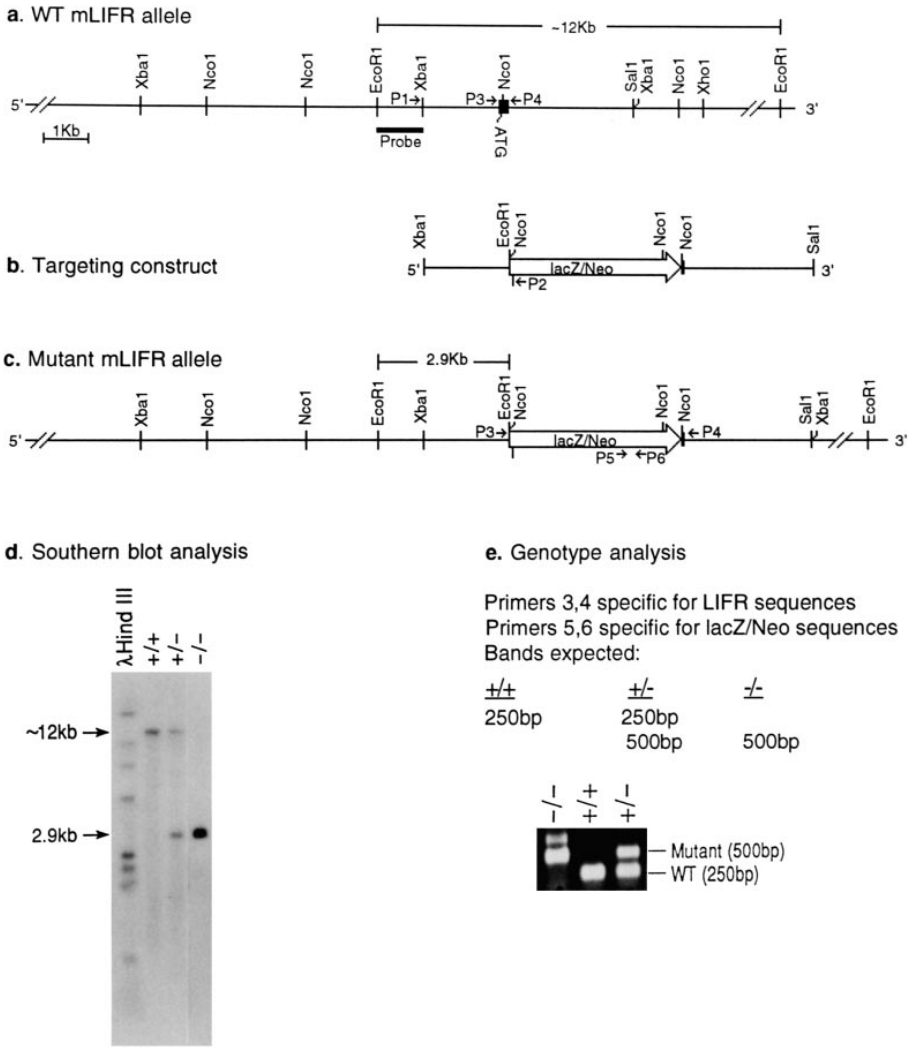

Fig. 1. Targeted mutation of the murine LIFR gene. (a) Schematic diagram of the wild-type allele. The start codon is indicated by ATG. The box labeled 'probe' represents the location of the probe used to detect restriction fragment length of genomic DNA on Southern blot analysis. (b) Gene targeting vector pMLIFR/ZN#1. (c) Diagram of the targeted mutant LIFR allele. (d) Southern blot analysis of the wild-type and mutant LIFR alleles. Positions of hybridizing bands are indicated (2.9 kb for the mutant allele and approximately 12 kb for the wild-type allele). (e) Genotype analysis of ear biopsy DNA. Positions of the oligos used for PCR analyses (P1-6) are indicated in panels a, b and c.

Table1. Genotype of offspring derived from LIFR +/– × +/– matings

	LIFR genotype			
	+/+ (%)	+/– (%)	–/– (%)	
Pups at 4 weeks	225 (36)	393 (64)	0	
Dead at birth	9 (35)	3 (11)	14 (54)	
Fetal day:				Resorbed (%)
3.5	39 (35)	53 (48)	19 (17)	
9.5-11.5	74 (30)	135 (55)	36 (15)	61/306 (20)
12.5-15.5	134 (35)	183 (48)	62 (17)	61/378 (16)
17.5-19.5	187 (31)	332 (54)	90 (15)	95/572 (17)
Fetal total	434 (32.3)	703 (52.3)	207 (15.4)	217/1256 (17)

or 6 hours (E13.5) washed with PBS and held in PBS at 4°C until frozen to −196°C. Three E11.5 and four E13.5 LIFR–/– fetuses were immunohistochemically compared with wild-type littermates, whereas two E10.5 and six E.11.5 LIFR–/– fetuses were compared with wild-type littermates by confocal microscopy. Whole-mount immunocytochemistry was carried out as described (Gomperts et al., 1994). Stained embryos were examined on a confocal laser scanning microscope (CLSM; Zeiss, Germany). All manipulations on the CLSM were according to the protocol described (Tsarfaty et al., 1992, 1994). Alkaline phosphatase immuno-histochemistry was carried out on frozen sections of embryos as described (Donovan et al., 1986).

Skeletal preparations were made on E18.5 Cesarean section derived fetuses as described (Gendron-Maguire et al., 1993). Briefly, the fetuses were eviscerated and fixed in 100% ethanol for four days followed by three days in acetone. They were then rinsed with water and transferred to staining solution which contained 1 volume of 0.1% Alizarin red S (Sigma 5533) in 95% ethanol. After staining for 10 days, the skeletons were rinsed with water, cleared with 20% glycerol in 1% potassium hydroxide overnight at 37°C and held at room temperature until cleared, at which point they were passed through 50, 80 and 100% glycerol for storage.

Mice were killed for histomorphometric analysis of bone from E17.5 to 19.5. The femora and tibiae were removed and stripped of soft and connective tissue and placed in 40% ethanol at 4°C then transferred 24 hours later to 70% ethanol. Bone samples were dehydrated in graded ethanols (40-100%) and cleared in toluene using a Tissue Tek VIP tissue processor (Miles Scientific, Naperville, IL). After dehydration and clearing, the bones were infiltrated in graded steps with methyl methacrylate at 4°C over 10 days. The bones were then transferred to scintillation vials containing a layer of prepolymerized methyl methacrylate, covered in fresh methyl methacrylate and left at room temperature for 16-24 hours. The vials were next placed in a radiant oven at 42°C for 2-3 days to allow for complete polymerization. The vials were removed, the blocks trimmed and sanded in preparation for sectioning. The blocks were cut into 4 μm longitudinal sections using a Reicher-Jung Autocut microtome (R. Jung, Heidelberg, Germany) with a tungsten-carbide blade. The sections were mounted on gelatin-coated slides and incubated overnight at 42°C. After deplastification, bones were stained with toluidine blue, pH3.7. Histomorphometric parameters (Parfitt et al., 1987) were analyzed by Osteomeasure software (Osteometrics, Atlanta, GA). All measurements were taken beginning at a standard point in the femur or tibia just below the growth plate and not including the diaphyseal area. Measurements were done on trabecular bone only and did not include cortical or endosteal bone surfaces.

Statistical analysis

Significant differences for MAP kinase activity and sensory neuron survival were determined by paired-sample *t*-test. Differences in the hematological assays were measured by chi-square (χ^2) or paired-sample *t*-test. Significant differences among groups analyzed histomorphometrically for bone formation and resorption were calculated by ANOVA (Scheffe F-test).

RESULTS

Homologous recombination of one allele with LIFR targeting vector in ES cells

LIFR is expressed in ES cells (Renshaw, unpublished observation); therefore, the targeting strategy incorporated a promoterless selection vector. One genomic clone was shown to contain the exon encoding the LIFR initiator methionine. A fragment, in which the ATG had been deleted, was subcloned with the intention of replacing the start codon via the lacZ/neo fusion cassette inserted just downstream of the deleted ATG.

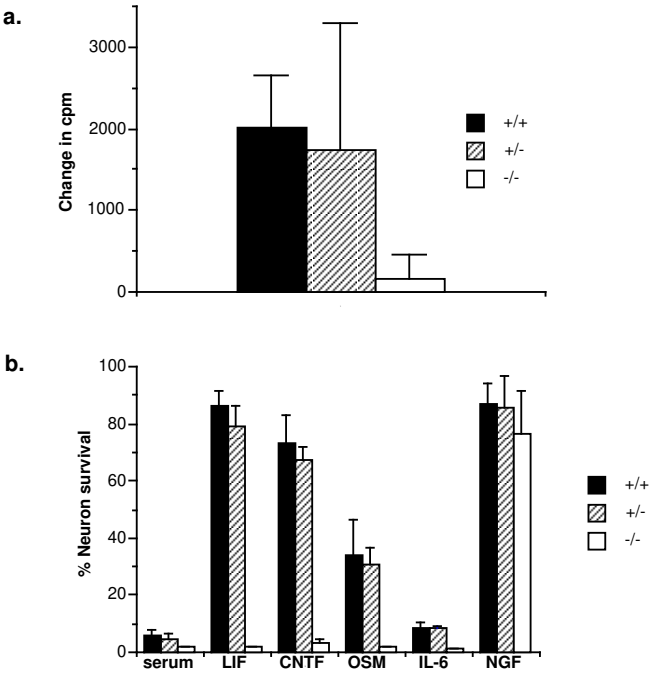

Fig. 2. Analysis of loss of gene function following targeted disruption of LIFR. (a) Combined data of LIF and OSM activation of MAP kinases in cultured cells derived from whole fetuses. Values are given as agonist induced (stimulated minus unstimulated) MAP kinase activity as measured by cpm of phosphate (^{32}P) incorporation in substrate peptide. Seven animals of each genotype were compared. Mean ± s.d. are shown for all three genotypes. The change in phosphate incorporation from baseline as a measure of MAP kinase activity for LIFR–/– cultures is significantly different when compared to combined data for LIFR+/+ and +/– MAP kinase activity (P<0.001, paired-sample *t*-test). (b) Response of differentiated DRG neurons from LIFR +/+, +/– and –/– perinatal mice to growth factors. The percentage neuronal survival was determined by counting the individual wells after 2 days. The graph includes data from two separate experiments with five replicate cultures per experimental condition, except OSM and IL-6 means which are combined data from one experiment. The data shown are mean ± s.d. of percent survival. Survival of LIFR–/– neurons was significantly different when compared to combined data for LIFR+/+ and +/– neuron survival (P<0.01, paired sample t-test).

The targeting vector contained 1.9 kb of homologous sequences 5′ of the selectable marker and 5.6 kb of 3′ homologous sequences (Fig. 1a-c).

After electroporation, G418 resistant clones carrying a LIFR allele disrupted by homologous recombination were identified by PCR using primers to detect incorporation of lacZ (P1 and P2) or to amplify the wild-type LIFR allele (P3 and P4) (Fig. 1a,b). Targeted clones were verified by Southern blot analysis (Fig. 1d). Five of fifteen G418 resistant clones carried a disrupted LIFR allele.

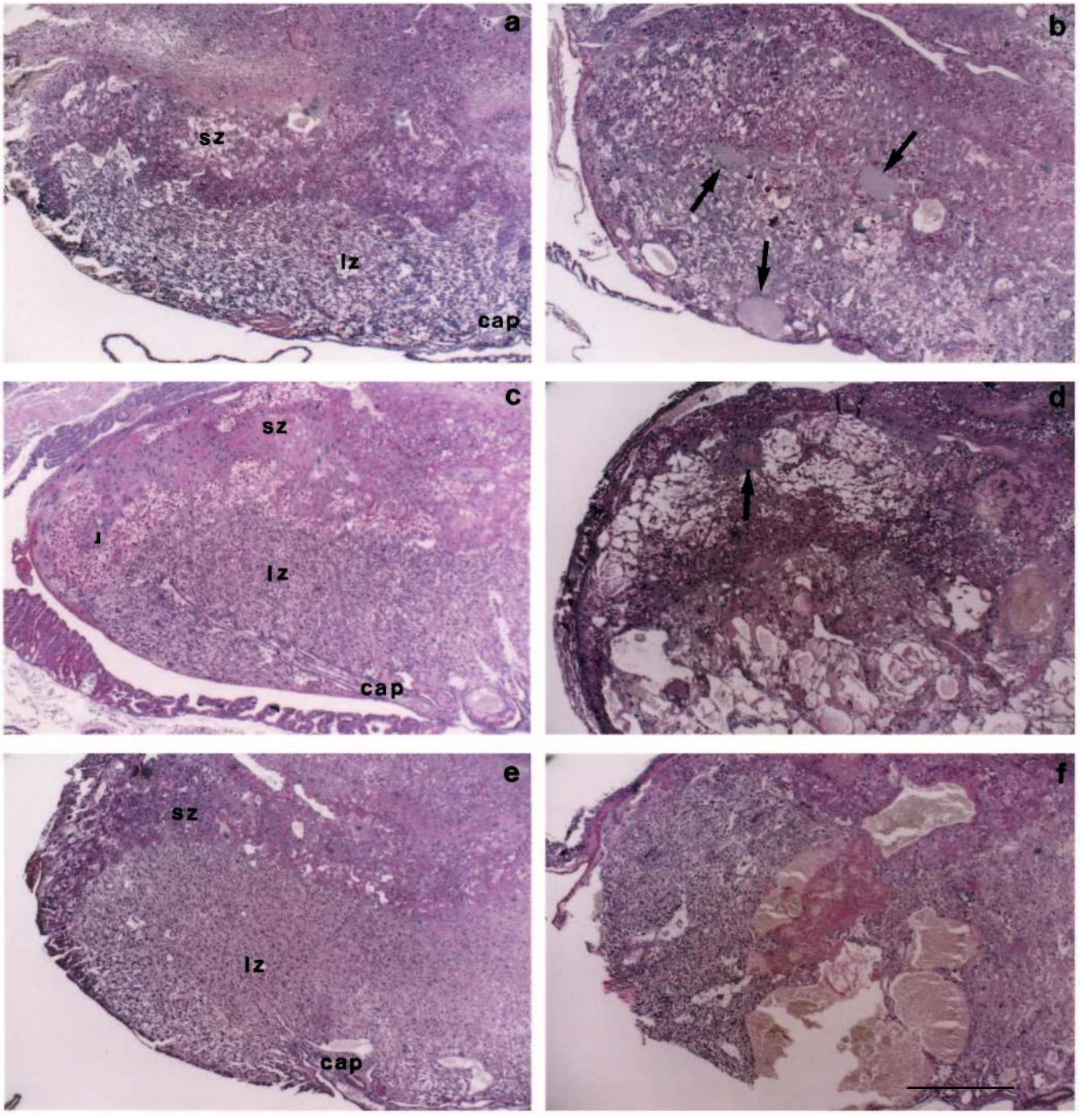

Fig. 3. Placentas from normal (+/+, +/–) and LIFR-deficient (–/–) embryos. (a) E13.5 +/+ embryo. Note that the placenta is clearly organized into a spongiotrophoblastic zone (sz) and labyrinthine zone (lz). Membranes that surround the embryo are attached at the chorioallantoic plate (cap), which forms the base of the placenta and is contiguous with the cord. (b) E13.5 –/– embryo. Note the lack of distinct organization into spongy and labyrinthine regions. Arrows point to large, fluid filled spaces in the labyrinthine region. (c) E15.5 +/– embryo. The placenta is well organized into distinct regions. (d) E15.5 –/– embryo. Note the lack of organization, edema and the presence of large fluid and blood-filled spaces in the labyrinthine region. An arrow marks an area containing multiple cell nuclei. (e) E17.5 +/+ embryo. The labyrinthine zone is lacy and a few large maternal blood spaces are present near the chorioallantoic plate. (f) E17.5 –/– embryo. The placenta is disorganized and edematous. Vast spaces filled with maternal blood are present, particularly near the chorioallantoic plate. PAS stains; size bar indicates 500 μm.

Generation of LIFR-deficient mice

One clone with a disrupted allele that had a normal karyotype by G-banding (Diagnostic Cytogenetics, Seattle, WA) was able to contribute to the coat color in two male chimeras. Offspring of matings between the chimeras and 129/J females were monitored by PCR of ear biopsy tissue for transmission of the LIFR mutation. The mutant allele was detected by amplification of the neo resistance gene (P5 and P6; Fig. 1c). Six of 20 male offspring from one chimera inherited the LIFR mutation. Four founder males were verified to be LIFR+/– by Southern

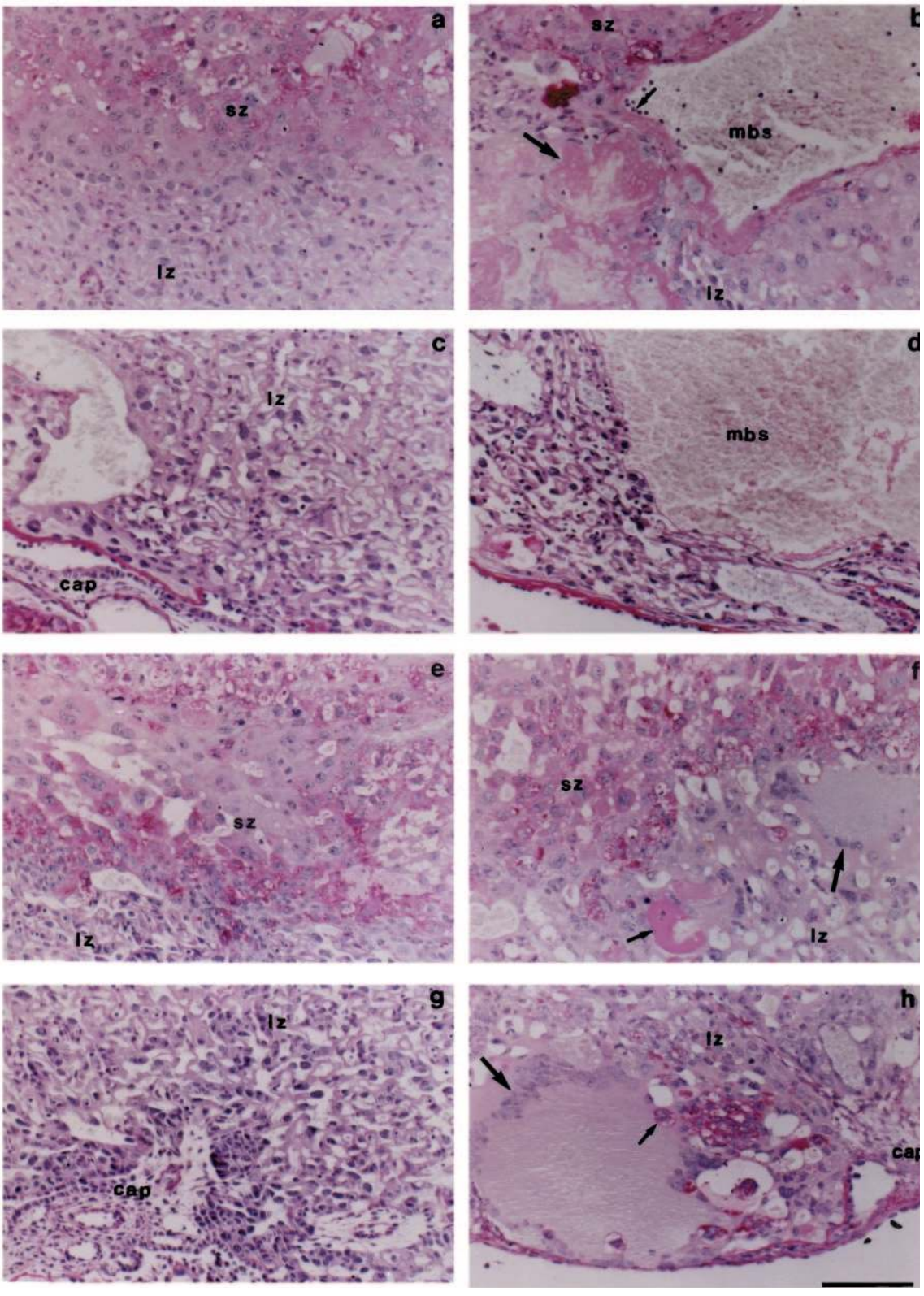

Fig. 4. Comparisons of the spongiotrophoblast/labyrinthine zone junctions and chorioallantoic plate regions of E17.5 and E13.5 normal and LIFR-deficient placentas. (a,c) E17.5 +/+ embryo; (b) and (d) E17.5 –/– embryo. (b) A large arrow points to fibrin and a small arrow points to a group of marginated leukocytes in a distended maternal blood space (mbs). (e,g) E13.5 +/+ embryo; (f,h) E13.5 –/– embryo; large arrows in point to PAS-negative areas that have indistinct borders and contain multiple cell nuclei. (f) A small arrow points to an accumulation of PAS positively staining material; (h) a small arrow points to an apparently intact PAS positively staining cell in one of these spaces. PAS stains: sz, spongiotrophoblast zone; lz, labyrinthine zone; size bar indicates 100 μm.

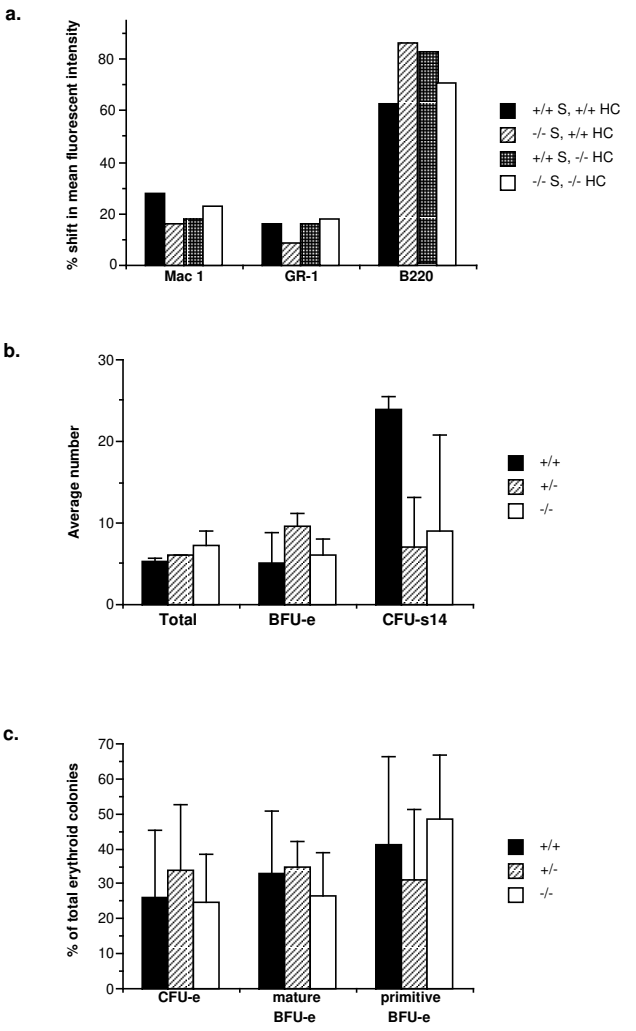

Fig. 5. Analysis of fetal liver hematopoiesis following targeted disruption of LIFR. (a) E18.5 fetal liver stromal support of E18.5 fetal liver hematopoiesis. The number of cells is determined by a shift in the mean fluorescence intensity as determined by FACS. There was no significant difference between genotypes for any of the combinations tested (χ^2). (b) E13.5 fetal liver cellularity, erythroid potential and CFU-s14 capability. Total cellularity (total cell number $\times 10^{6)}$ of E13.5 fetal livers was determined for each genotype. BFU-e numbers were determined following culture in methylcellulose. CFU-s14 colonies were determined by counting fixed spleen surface colonies. Mean ± s.d. are shown for all three genotypes. There was no significant difference between the genotypes for any of the parameters tested (paired-sample *t*-test). (c) E15.5 erythroid morphology. The number of colonies of each erythroid compartment from CFU-e (most mature) to primitive BFU-e (least mature) were counted following culture and are represented as percentage of the total erythroid colony outgrowths. Mean ± s.d. are shown for all three genotypes. There was no significant difference between any of the genotypes (χ^2).

blot analysis. Matings were arranged to carry the LIFR mutation on both inbred and outbred backgrounds. Birth of litters from 129 strain LIFR+/– mating pairs was rare. Thus, founder males mated to C57BL/6 females were the source of subsequent generations carrying the mutation. The genotypes of animals generated from +/– × +/– matings were detected by either PCR (P3 and P4, to amplify the unaffected LIFR allele, plus P5 and P6, to amplify the neo resistance gene in the targeted allele) (Fig. 1).

Genotypes of pups and fetuses derived from LIFR+/– × +/– matings are represented in Table 1. There were no LIFR–/– mice detected in PCR analysis of blood tissue taken from 4-week-old pups from LIFR+/– × +/– matings. Otherwise +/+ and +/– pups were represented by close to Mendelian ratios (36% +/+ versus 64% +/–). Pups found dead within a few hours of birth (P1) were analyzed by leg biopsy. 14 of 26 pups were LIFR–/– as confirmed by Southern blot analysis (Fig. 1d).

Pregnancies generated from LIFR+/– × +/– matings were disrupted on days 3.5 and 9.5 to 19.5 of gestation to determine the percentage of LIFR–/– fetuses present (Table 1). The number of LIFR–/– fetuses from E9.5 to 11.5 is less than expected (15% observed versus 25% expected). The genotypes of E3.5 embryos were also skewed (17% observed versus 25% expected) indicating that the underrepresentation of LIFR –/– embryos may exist prior to implantation. A subtle overrepresentation of LIFR +/+ animals is also present throughout gestation (32% observed versus 28% expected). After implantation there was evidence of excessive fetal resorption (17%) as determined by counting resorption points contained within the uterus. Advanced resorptions could not be genotyped accurately due to the predominance of maternal tissues; however, all genotypes of LIFR are represented during early resorption (data not shown). Non-resorbed LIFR–/– fetuses were visually indistinguishable from their littermates.

Because LIFR–/– fetuses were present at a late stage of pregnancy, pups were obtained by Cesarean section on E18.5 and placed with foster mothers to determine whether stress of vaginal delivery was associated with perinatal death. No LIFR–/– pups survived beyond the day of Cesarean birth (P1). 9 of the 13 LIFR–/– pups that were delivered by Cesarean section died within 1.5 hours of delivery. These pups appeared grossly normal but lacked vigor and were often rejected by the foster mothers, as were the rare survivors of vaginal delivery. The other four pups were accepted by the foster mothers but died 6-16 hours after delivery although they were indistinguishable from their littermates in their overall vigor during the first few hours of life. However, their stomachs contained only white froth, whereas most of their littermates had milk in their stomachs. All LIFR+/+ and +/– animals that were accepted by the foster mother thrived. Several LIFR–/– animals appeared smaller than their wild-type or heterozygous littermates; however, not all LIFR–/– animals were relatively small and small LIFR+/+ and +/– animals were observed.

Analysis of loss of LIFR function in fetal LIFR–/– fetuses

MAP kinase activity

MAP kinases become activated in a variety of cell types in response to LIF and OSM (Thoma et al., 1994). This activity was exploited to establish that the introduced LIFR mutation was, in fact, a functionally null mutation. The induction of MAP kinase activity in response to treatment with LIF or OSM was assessed in cells derived from E12.5 and E15.5 LIFR+/+, +/– and –/– fetuses to determine loss of LIFR function. Cells from dissociated embryos were cultured to confluence and stimulated with OSM, LIF or PMA, which served as a positive control for stimulation of MAP kinase activity in all cultures. MAP kinase activity in unstimulated cells from all three

Table 2. Bone histomorphometry of LIFR +/+, +/– and –/– mice

Parameter	Phenotype +/+ (*n*=5)	+/– (*n*=7)	–/– (*n*=9)	Ratio –/–:+/+	–/–:+/-	+/–:+/+
Bone volume (%)	13.4±0.9	15.2±0.2	4.8±0.6a	0.4	0.3	1.1
Osteoid volume (%)	2.2±0.7	2.5±0.4	1.4±0.4	0.6	0.6	1.1
Osteoid surface (%)	3.5±1.1	4.1±0.5	2.6±0.7	0.7	0.6	1.2
Osteoid thickness (μm)	1.7±0.09	1.6±0.07	1.5±0.2	0.9	0.9	0.9
Osteoclast surface (%)	0.6±0.3	0.7±0.2	4.1±0.6a	6.9	5.9	1.2
Number of osteoclasts/mm^2	0.3±0.2	0.4±0.1	1.8±0.2a	6.1	4.6	1.3

Data are presented as means of numbers in each group ± standard errors.
[a]Indicates significance at P<0.001 as determined by ANOVA. Significant differences (ratio) were only observed between homozygous mutant mice (–/–) and either wild-type (+/+) or heterozygous mice (+/–).

genotypes was comparable (average: 2360±786 cts/minute), and the change of MAP kinase activity from this baseline activity upon stimulation with the agonists is shown in Fig. 2a. PMA was able to induce activation of MAP kinases in cells from all genotypes (average induced MAP kinase activity: +/+ 6935 cts/minute, +/– 7224 cts/minute and –/– 5432 cts/minute). LIF and OSM stimulated MAP kinase activation significantly in LIFR+/+ and +/– cells (average induced MAP kinase activity: +/+ 2003 cpm, +/– 1736 cpm), whereas in LIFR–/– cells neither LIF nor OSM were able to appreciably stimulate MAP kinase activation (average: 156 cts/minute).

Sensory neuron survival

The ability of E19.5-20.5 LIFR–/– DRG derived sensory neurons to survive after two days of in vitro culture in the presence of cytokines that use LIFR to mediate survival was explored as additional evidence of a null mutation of LIFR. Because neurons derived from animals older than E18.5 were preferred for this assay, parturition was delayed with progesterone for 24 hours to obtain E19.5 fetuses. E20.5 fetuses were recovered on the day of natural parturition (E20.5=P1). The cells from the E19.5 fetuses were cultured in either serum alone or serum supplemented with NGF, LIF, CNTF, OSM or IL-6. The E20.5 (P1) DRG cells were cultured in either serum alone or serum supplemented with NGF, LIF or CNTF. None of the cultures survived in either IL-6 or serum alone, whereas all survived in NGF regardless of genotype. As expected, the +/+ and +/– sensory neurons survived in the presence of cytokines that are known to use LIFR to mediate signal transduction events (LIF, CNTF, or OSM), whereas sensory neurons from the LIFR–/– littermates did not survive in the presence of these cytokines (Fig. 2b).

LIFR null ES cell lines

We have been unable to derive ES cell lines carrying targeted disruptions of both LIFR alleles. Repeated attempts at deriving LIFR null ES cell lines by either transfection of LIFR+/– lines with a second targeting vector or by selection of LIFR+/– lines in elevated G418 levels as described (Mortensen et al., 1992) have failed (data not shown). These data argue that LIFR is required for suppression of ES cell differentiation by LIF and, taken with the above data, that the targeted LIFR alteration is indeed a null mutation.

LIFR–/– fetuses displayed disrupted placental architecture

The only grossly detectable defect observed in LIFR–/– fetuses was the presence of blood lacunae on some of the associated placental/decidual/metrial gland units (maternal-fetal interface); therefore, we looked at placental development. Maternal-fetal interface units were sectioned and stained by PAS to discern if this phenomenon was unique to LIFR–/– fetuses. Blood pooling was seen to some extent in placentas from all genotypes; however, the pools were dramatically larger in the LIFR–/– placentas, which often extended from the spongiotrophoblast, the placental tissue nearest the maternal decidua, down to the chorioallantoic plate (Figs 3f,4b). LIFR mutant placentas were edematous, with large fluid-filled spaces, and lacked organization into distinct spongio- and labyrinthine trophoblast zones (Fig. 3b,d,f). In contrast, placentas from LIFR+/+ and +/– fetuses were clearly organized (Fig. 3a,c,e). Mutant placentas contained unusual pale grey, PAS-negative structures resembling multinucleated cells with indistinct cell borders and aggregates of nuclei (Figs 3b, 4f). Some of these structures also contained intact PAS-positive cells that were either spongiotrophoblast cells or maternal natural killer-like cells (Fig. 4h). E17.5 placentas contained excess fibrin in association with the blood lacunae, and marginated leukocytes could be detected in some of these enlarged maternal blood spaces (Fig. 4b). Multinucleated cells and fluid-filled spaces of the E13.5 and 15.5 placentas were uncommon by E17.5. The characteristic lacy appearance of the normal labyrinthine placenta was lost by E17.5 due to thickening of either the trophoblast or the underlying mesenchyme.

Fetal hematopoiesis is relatively normal in LIFR–/– mice

Functionality of mutant fetal liver cells to support hematopoiesis was assessed three ways: in vitro stroma culture support of hematopoiesis, spleen colony formation assay and erythroid outgrowth from fetal livers to compare the ability of mutant versus wild-type fetal liver stroma to support growth of mutant versus wild-type hematopoietic cells. Irradiated fetal liver adherent stroma layers were reseeded with freshly isolated E17.5 fetal liver cells. Cultures were supplemented with IL-7 and SLF, a combination known to induce both myeloid and B cell development under these culture conditions. The number of cells after culture was elevated more than six-fold when wild-type cells were cultured on a LIFR–/– stroma as compared to the other three groups (data not shown). Outgrowths from these cultures were assayed by flow cytometry to compare relative populations of Mac-1$^+$ cells (macrophage lineage), GR-1$^+$ cells (granulocyte lineage) and

B220+ cells (B cell lineage). There was no significant difference in the lineage phenotypes observed in the different genotype combinations tested (Fig. 5a).

Primitive progenitor cells derived from fetal liver were assessed by determining the frequency of spleen colony formation on day 14 (CFU-s14). Cells from individual livers were cultured overnight in IL-3 and SLF, a combination of cytokines previously shown to support the short-term survival of cells capable of forming colonies (McKenna, unpublished data). The total cell number per liver did not differ significantly among the LIFR genotypes (Fig. 5b). After overnight culture, the cells were injected intravenously into lethally irradiated

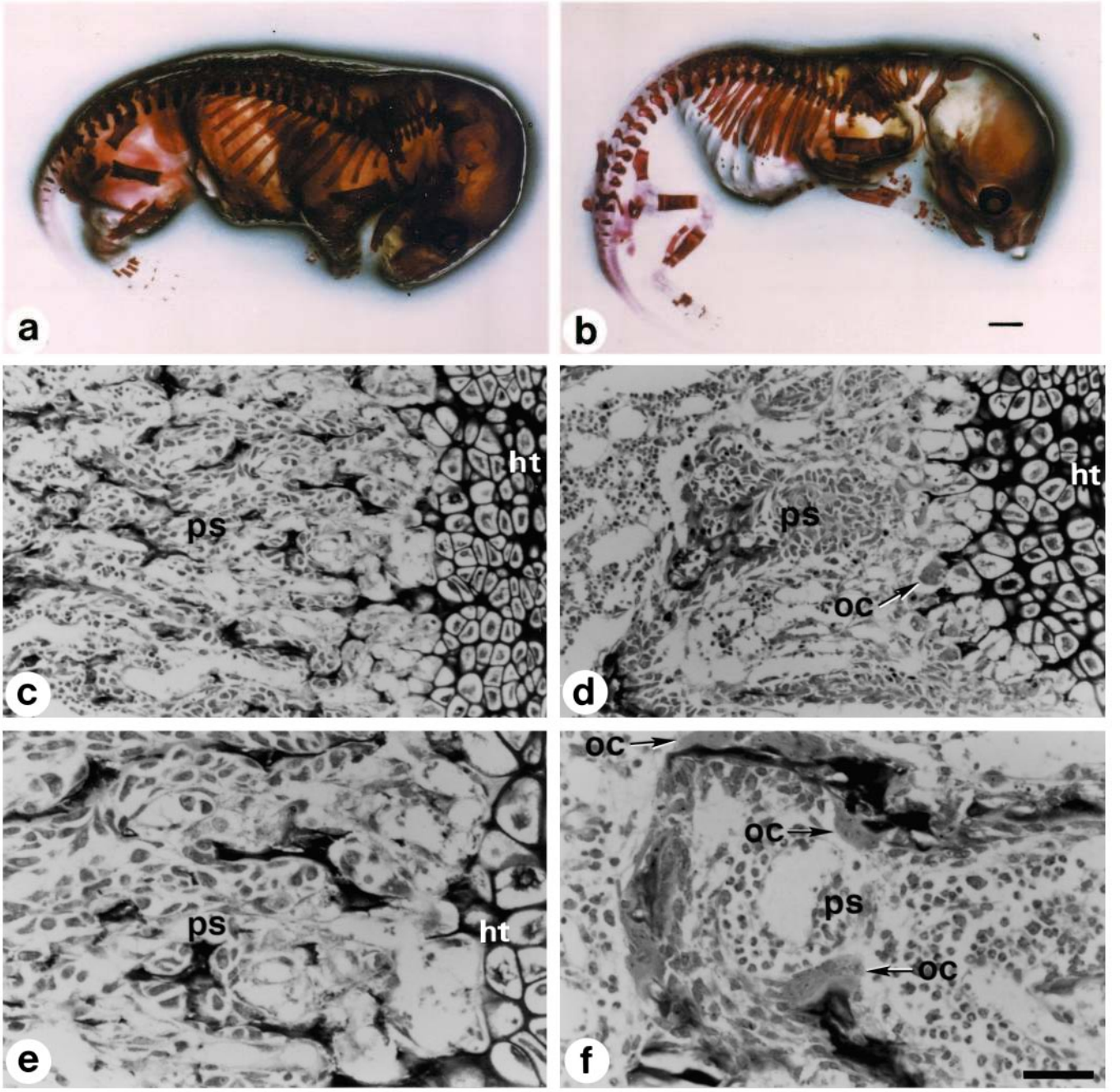

Fig. 6. Bone development abnormalities in LIFR-deficient animals. E18.5 wild-type (left) and mutant (right) fetuses. (a, b) Whole Alizarin red-stained fetuses. Note the reduction in bone density throughout the mutant animal, which is especially apparent near the growth plate in long bones. (c-f) The proximal tibial growth plate by light microscopy of the hypertrophic region of the growth plate (ht) and primary spongiosa (ps). (c,d) Note the marked reduction in bone spicules and complete absence of trabeculae in the mutant as compared to the wild-type mice. Osteoclasts (oc) can be observed at the interface between the hypertrophic zone and the primary spongiosa in mutant but not wild-type mice. (e,f) The proximal tibial growth plate and the primary spongiosa of the wild-type and mutant at higher magnification. In the mutant, note the large numbers of osteoclasts lining the bone surfaces which are absent in the wild-type bone. Size bar (b) indicates 1.5 mm in a and b. Size bar in lower right indicates 3 mm in a and b, 80 μm in c and d, and 40 μm in e and f.

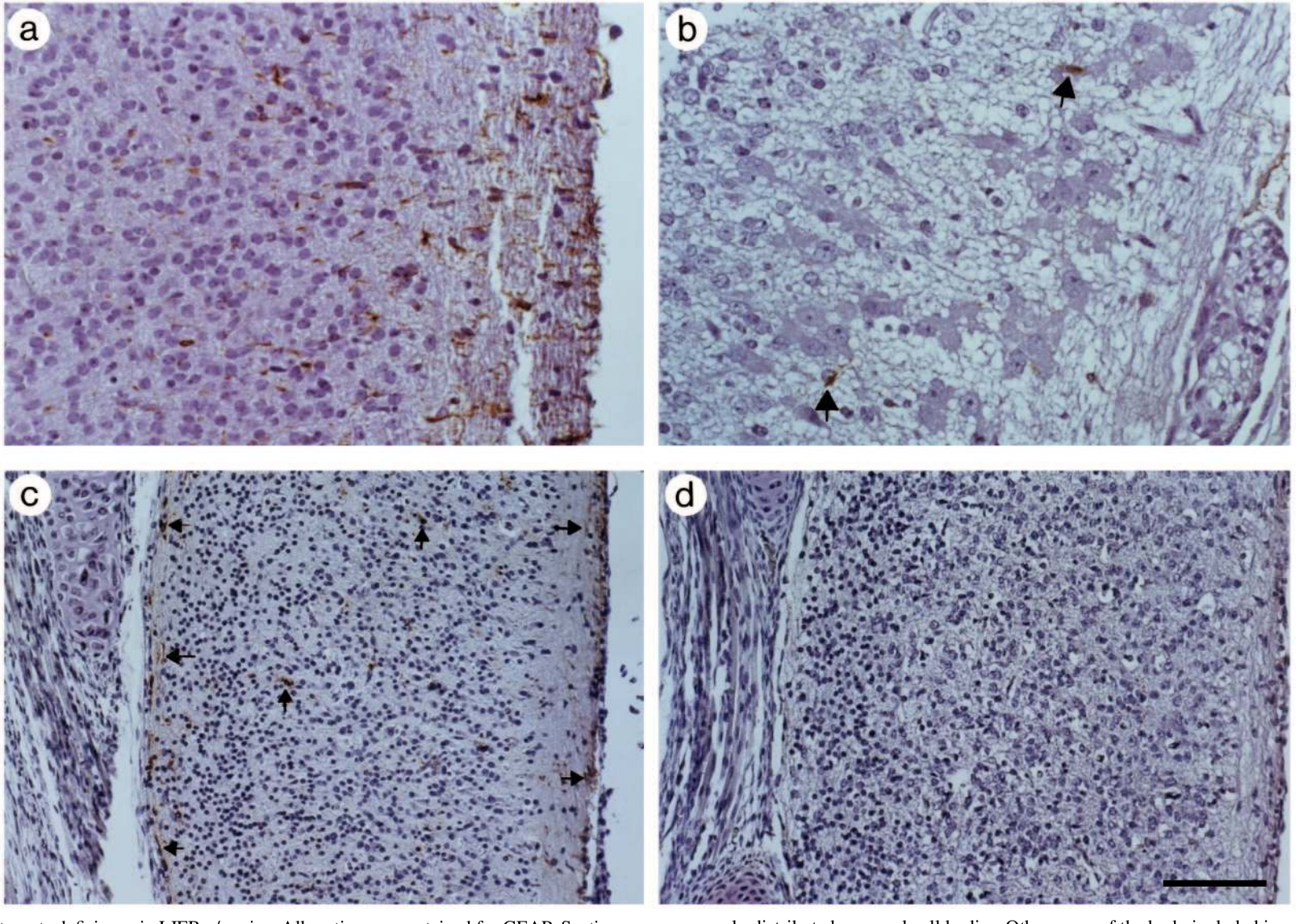

Fig. 7. Astrocyte deficiency in LIFR –/– mice. All sections were stained for GFAP. Section of spinal cord from an E17.5 LIFR+/– fetus (a) and an E18.5 LIFR +/+ fetus (c). Positively stained cells (brown) are seen in the outer marginal layer with fewer in the inner portions of the neuron-rich mantle layer. Arrows in c highlight a few of the many GFAP-positive cells. (b) Spinal cord section from an E17.5 LIFR–/– fetus. Two positively stained cells are visible in the mantle layer (arrows) where they are separated by vacuolated neuropile and unevenly distributed neuronal cell bodies. Other areas of the body included in sections from this animal had good tissue integrity. (d) Spinal cord section from a E18.5 LIFR –/– fetus. Note the absence of GFAP positively stained cells and the abnormal neuropile and neuronal cell body distribution. All sections are sagittal. Sections in a and b are 4 µm thick whereas sections represented in c and d are 7 µm thick. Size bar indicates 25 µm in a and b, and 87.5 µm in c and d.

C57BL/6 × 129 hybrid adult hosts. After 14 days the number of macroscopic CFU-s14 colonies was determined. No significant difference in CFU-s14 was observed, though considerable variation in frequencies was apparent (Fig. 5b). Numbers of committed erythroid progenitor cells in the fetal livers were assessed by determining the frequency of erythroid burst forming units (BFU-e) after culturing in methylcellulose of an aliquot of the same fetal liver cells used to determine CFU-s14. No significant difference in the frequency of BFU-e colonies was seen among the three genotypes after 7 days of culture in methylcellulose (Fig. 5b).

Erythroid developmental morphology was evaluated following outgrowth of fetal liver cells in methylcellulose to ascertain the stage of hematopoietic development in light of the severe placental disruption observed. There was no significant difference in maturity of erythroid colonies observed among the genotypes (Fig. 5c). There was an insignificant tendency toward a more primitive morphology in the LIFR–/– animals, but it was below the limits of detection of this assay and was not considered physiologically relevant.

LIFR–/– animals have decreased bone volume and increased osteoclast numbers

Adult mice respond to excess circulating LIF by increased osteoblast numbers that result in mineralized bone overgrowth (Metcalf and Gearing, 1989a,b); therefore, the absence of LIFR could affect bone formation and resorption. Fetuses were stained with Alizarin red S to detect mineralized bone (Fig. 6a,b). The mutant animals cleared noticeably faster and more thoroughly than their +/+ or +/– littermates after Alizarin red S staining. The skin was not removed from any of the animals and may have contributed to the differential tissue clearing. As stated above, the LIFR+/+ mice tend to be larger than their –/– littermates. Skull bones, vertebrae and ribs in the mutant mice are noticeably less dense. One of the most striking features of the LIFR–/– mice is the loss of density at the proximal and distal ends of the long bones and metacarpi. In order to evaluate bone remodeling, the femora or tibiae from E17.5-19.5 fetuses were processed for histomorphometric analysis and evaluated by light microscopy. Histomorphometric measurements were performed on a fixed region just below the growth plate (primary spongiosa) (Baron et al., 1984). Bones from wild-type and heterozygous mice were normal for this stage of development and indistinguishable from each other. The primary spongiosa contained numerous mineralizing spicules extending distally from the cartilaginous growth plate, which also appeared normal. These spicules formed the finger-like projections of the trabeculae and the resulting bone architecture was well organized (Fig. 6c,e). Cortical bone was of normal thickness and the bone marrow was unremarkable.

In contrast, the skeletons of homozygous mutant mice exhibited profound changes. The most striking feature was the loss of bone, assessed by histomorphometric analysis, which was reduced by approximately two thirds as compared to controls (Table 2). Although there appeared to be a generalized decrease in bone mass, the loss was most evident in the primary spongiosa, which was distinctly osteopenic, with reduced numbers of bone spicules and few if any well-formed trabeculae (Fig. 6d,f). This resulted in the failure to develop the normal architecture observed in control mice. The majority of bone loss may be accounted for by the six-fold increase in osteoclast numbers and the seven-fold increase in osteoclast surfaces (Table 2). Numerous osteoclasts were observed attached to the few bone spicules found in the primary spongiosa and at the interface between the calcified cartilage and the primary spongiosa in mutant animals (Fig. 6f). Bone formation may also be affected as indicated by a decrease (~33%) in osteoid volume. Although this decrease was not statistically significant, the trend would contribute to the overall decreased bone mass. However, once bone formation commenced there was no difference observed between mutant and control mice as reflected in osteoid thickness. The developing cortical bone appeared normal, although there was less bone radiating from midshaft to the epiphysis.

LIFR–/– animals have fewer spinal and brainstem astrocytes

The structures of the central nervous system of LIFR–/– animals appeared normal or had slightly reduced staining intensity as viewed in 4-7 μm sections of whole animals stained with hematoxylin and eosin. It had been observed that upon culture of neuroepithelium derived from E10.5 LIFR–/– fetuses, astrocyte outgrowth was less than 1% that seen in neuroepithelium outgrowths of littermates (Koblar, unpublished observation). Therefore, we stained fetal sections with an antibody to GFAP, an astrocyte-specific stain. The astrocyte numbers in the spinal cord and brain stem, as detected with GFAP, were noticeably reduced in all spinal sections from E17.5-18.5 LIFR–/– fetuses as compared to their +/+ and +/– littermates (Fig. 7). E12.5 and 15.5 fetuses were negative for GFAP regardless of genotype. Staining for GFAP was most noticeable along the outer edge of the marginal layer of the spinal cord in the wild-type littermates by E17.5 with scattered staining toward the center of the mantle layer (Fig. 7a). This effect was accentuated on E18.5 (Fig. 7c). Extremely rare cells on the outer marginal layer of the spinal cord stained for GFAP in the LIFR–/– E17.5 and 18.5 animals and, though numbers were strikingly reduced, a few positively stained cells were within the mantle layer (Fig. 7b,d). Interestingly, the neuronal population appeared to be affected as viewed by the counterstain. The area between neuronal bodies appeared abnormal in that the processes were thickened and tangled, whereas neuron bodies containing cytoplasmic vacuoles and condensed, pyknotic nuclei were scattered throughout the field (Fig. 7b,d). The lesions involved the spinal cord and extended into the brain stem, the same area where GFAP staining was prominent in the wild-type littermates and may reflect a deficit in neuronal survival.

Primordial germ cells are unaffected by the LIFR mutation

We examined PGC numbers in LIFR–/– embryos ranging in age from 10.5 to 13.5 days post coitus. PGC numbers were examined in whole mounts by staining with a monoclonal antibody that recognizes PGC followed by analysis with confocal laser scanning microscopy or by alkaline phosphatase immuno-histochemistry on frozen sections. No differences could be detected in the PGC populations among genotypes either in number or gross morphology (data not shown).

Elevated glycogen in the E18.5 LIFR–/– fetal liver

LIF has been reported to be involved in metabolism (Metcalf

and Gearing, 1989a; Mori et al., 1989). While histologically examining placentas, we noticed that PAS staining of sectioned, whole fetuses highlighted an increase in stored glycogen in the E18.5 LIFR–/– fetal liver relative to wild-type littermates (Fig. 8). The difference was subtle on E17.5 and was not detectable on E15.5 or earlier. After Cesarean section, the glycogen stores of all genotypes were rapidly metabolized and could no longer be detected, thus ruling out a glycogen storage disease and suggesting elevated fetal circulating sugar levels (data not shown). Because the mutant mice die during a period of metabolic switch from maternal to self-support, study of metabolic defects in LIFR–/– animals is complicated by maternal and placental influences.

DISCUSSION

The LIF–/– mutation causes a defect in the uterine endometrium that disallows implantation (Stewart et al., 1992). Normal implantation of LIFR–/– embryos indicates that a direct uterine LIF-embryonic LIFR interaction is not required for implantation but suggests LIF and LIFR are members of a uterine cascade of events that allows implantation. Whether LIFR is an obligatory member of this cascade cannot be answered definitively because LIFR–/– animals do not reach reproductive age.

LIFR was cloned from a human placental cDNA library (Gearing et al., 1991), and the data presented here emphasize the requirement for LIFR in placentation. Maternal blood pooling in the placental labyrinth is a normal process that facilitates nutrient exchange to the fetus. However, the extent of pooling seen in the LIFR mutant animals is extreme. Very few vessels containing nucleated, fetal red cells were observed in the LIFR–/– placentas indicating a reduction in the fetal vascular component when compared to those of the wild-type littermates (Hunt, unpublished observation). There is precedent for LIF effects on the cardiovascular system (Ferrara et al., 1992; Gillett et al., 1993; Kirby et al., 1993; Lecron et al., 1993; Moran et al., 1994). The placentas of mice and humans contain essentially the same basic maternal and fetal cellular elements and perform the same functions but exhibit important structural differences. It is therefore difficult to draw exact parallels between the morphological alterations in murine LIFR mutant placentas and aberrant conditions of human pregnancy. However, large maternal chorionic blood spaces are a feature of placentas from mothers with certain metabolic diseases such as diabetes and may also be observed in severe preeclampsia (W. P. Faulk, personal communication). The accumulation of placental fibrin as gestation advances is a normal feature of pregnancy and is thought to aid in successful separation of the fetus from the mother at parturition. The excess accumulation of fibrin in the LIFR–/– placentas may have caused premature separation of the mutant fetuses during the events leading to vaginal delivery, which would result in death by hypoxia of the majority of the LIFR–/– animals prior to birth.

Previous reports that describe the requirement for SLF, LIF and bFGF either alone or in various combinations for in vitro primordial germ cell development focused on cells isolated from E8.5-11.5 genital ridges (De Felici and Dolci, 1991; Dolci et al., 1991; Matsui et al., 1991; Resnick et al., 1992). Neutralizing antibodies to LIFR block PGC survival in culture (Cheng et al., 1994) consistent with data to support that LIF can inhibit apoptosis of cultured PGCs (Pesce et al., 1993). That PGC numbers are normal in LIFR–/– mice suggests either that the antisera used in the previous study cross react with another molecule that is itself able to bind LIF (and other related cytokines) or that cytokine binding to gp130 alone is sufficient for PGC survival. Because the LIF-related cytokine OSM can also stimulate PGC proliferation in culture, binds directly to gp130 and is thought to have its own accessory receptor subunit, either of these explanations is plausible. The combination of noticeable loss of the expected number of LIFR–/– fetuses throughout gestation, an overrepresentation of LIFR+/+ animals, normal LIFR–/– PGC appearance and the apparent lack of a gene dose effect suggests that LIFR-deficient germ cells may be at a subtle disadvantage after removal of gap junctional support provided within the parental LIFR+/– gonads. Evaluation of late gestation LIFR–/– gonads should help reveal the role of LIFR in germ cell development.

Bone resorption and formation is a dynamic balance between the function of osteoclasts and osteoblasts. Osteoblasts secrete LIF and express LIFR, whereas equivalent functions have not been detected in osteoclasts (Allan et al., 1990). A role for LIF in osteoblast development is suggested by its ability to potentiate or inhibit the expression of alkaline phosphatase and type I collagen synthesis, depending on the cells or assay used (Lorenzo et al., 1990). Hormones known to stimulate bone resorption may also affect the production of cytokines, like LIF, by osteoblasts (Greenfield et al., 1993). LIF is known to induce bone resorption in cultured mouse calvaria via a prostaglandin-mediated mechanism (Reid et al., 1990), whereas excess LIF can inhibit bone resorption in E17 mouse metacarpal cultures, presumably due to an inability of the fetal osteoclasts to migrate from the periosteum into the mineralized bone (Van Beek et al., 1993). These differences may also be attributed to the stage of differentiation of the cells present in the organ culture.

The bone loss associated with postmenopausal osteoporosis is due in large part to the decrease in estrogen. Estrogen appears to function as a regulatory agent to maintain a balance between resorption and formation (Horowitz, 1993). Loss of the estrogen receptor, similar to the loss of the LIFR, results in increased bone loss (Smith et al., 1994). IL-6 has been implicated in the increased development of osteoclasts through its hematopoietic activity, particularly after the loss of estrogen (Jilka et al., 1992). IL-6-deficient mice appear to be protected from osteoporosis because they do not lose bone in response to estrogen loss following ovariectomy, although they retain elevated bone turnover rates (Poli et al., 1994). IL-6 uses two gp130 molecules, rather than LIFR and gp130, as its receptor signaling components, suggesting that gp130 may be important in the disease process. However, data presented here indicate that LIFR and possibly other receptor components may play equally important roles and that other cytokines, some of which have yet to be defined, may also use this receptor and therefore be involved in the osteopenia seen in the LIFR–/– animals. It would be interesting to explore the role of LIFR in comparison to gp130 for effects on osteoporosis. Furthermore, it can be predicted from the phenotype of the LIFR mutant animals that either reduction of LIFR expression or an increase in the release of soluble receptor localized to bone would, in

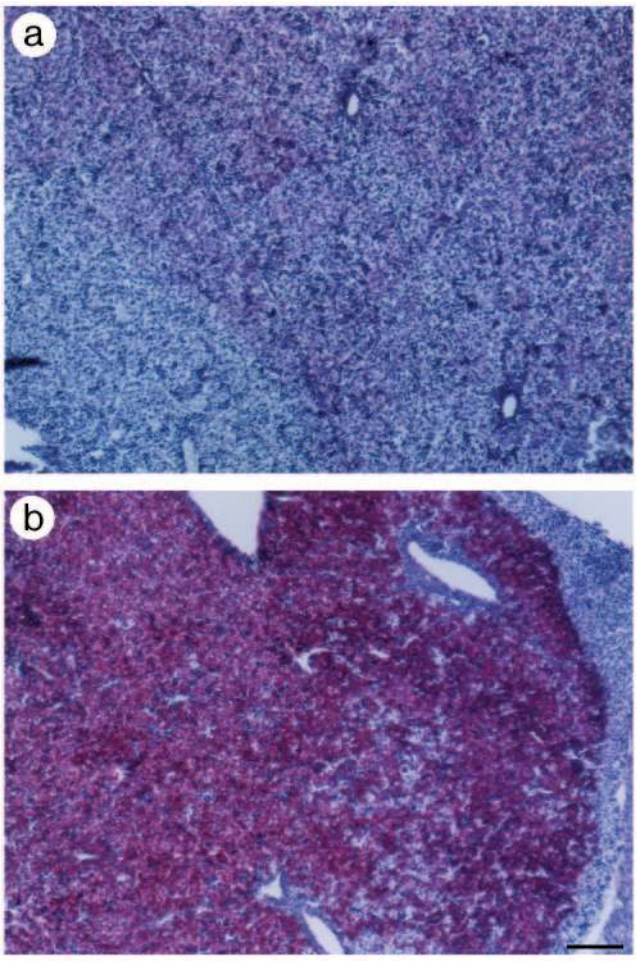

Fig. 8. Elevated glycogen levels in the LIFR–/– liver. (a) LIFR+/+ E18.5 fetal liver. Note faint staining (fuchsia) of glycogen granules. (b) LIFR–/– E18.5 fetal liver. Note dense staining of glycogen granules. Livers were fixed in paraformaldehyde, sectioned to 7 μm and stained by PAS. Size bar indicates 100 μm.

adult life, affect this equilibrium via the autocrine circuit of LIF secretion and utilization by osteoblasts. Because osteoblasts regulate osteoclastic activity (Thomson et al., 1986), the predicted outcome of these defects would be osteoporosis.

Studies in vitro have suggested multiple roles for LIF and CNTF in development of primary sensory neurons, including regulation of survival and differentiation of neurotransmitter properties (Nawa and Patterson, 1990; Ip et al., 1991; Murphy et al., 1991; Rao et al., 1992; Fan and Katz, 1993). LIF inhibits expression of the catecholamine-synthesizing enzyme tyrosine hydroxylase (TH) in dissociate cultures of fetal rat sensory ganglia and may play a similar role in inhibiting catecholaminergic differentiation in most sensory neurons in vivo (Fan and Katz, 1993). However, comparison of TH-immunostaining in the trigeminal and nodose sensory ganglia of E13.5, 17.5 and 18.5 LIFR +/+ and –/– mice revealed no apparent difference in the number of catecholaminergic sensory neurons (Fan and Katz, personal communication). Although LIFR is required for the regulation of neuron survival within the spinal cord during late gestation, signaling pathways involving LIFR are not required for inhibition of catecholaminergic differentiation during sensory gangliogenesis in vivo, suggesting that other mechanisms subserve this function in the LIFR mutant animals and perhaps during normal development.

Roles for both LIFR and gp130 astrocyte development are indicated by the observation that serum-free mouse embryo cells are stimulated to make GFAP in response to LIF, CNTF, OSM or IL-6 (Nishiyama et al., 1993). LIF is made by human fetal astrocytes (Aloisi et al., 1994) and rat glial cells (Banner and Patterson, 1994). Thus, murine astrocytes are likely to express LIF and these data suggest that they require LIFR either directly or indirectly to express GFAP. Because a biological clock determines glial development (Abney et al., 1981), the paucity of astrocytes found in the mutant animals may not be due to a simple delay in development, although the developmental clock is being examined for alterations in these mice. Whether the apparent inability of spinal neurons to survive is due directly to regulation by LIFR or is related to the reduction in astrocyte numbers is a question for future investigations.

We expect that there may be defects in LIFR–/– mice that have not yet been investigated such as skin formation and vascular development. The defects observed are severe in comparison to individual CNTF and LIF mutations. Breeding CNTF-deficient mice with mice lacking LIF and comparing these progeny with CNTFRα-deficient mice and mice lacking LIFR may reveal the presence of other ligands or receptors that directly or indirectly require LIFR to signal. It is surprising that there is so little redundancy in LIFR function. It is likely that the entire family of molecules, which transduce a signal through LIFR and/or gp130, is in the process of active evolution. As a result, we may predict that species variation occurs in both ligand and receptor components of this family.

The authors would like to thank Randy Hall for his attention to detail during mouse handling, Jeff Meyer and Betty Nakamoto for expert technical assistance, Kim Stocking for assistance in creating chimeras, Gayle Callis for trustworthy histology advice, Kam Au at Diagnostic Cytogenetics for producing reliable and thorough karyotypes, Anne Bannister for informed manuscript preparation, Nancy Troiano and Richard Darrell for their expert preparation and analysis of the bone histomorphometry, Roland Baron for his help in analyzing the data, David Anderson for advice regarding pathology, Tom DeChiara and George Yancopoulos for helpful discussion.

REFERENCES

Abney, E. R., Bartlett, P. F. and Raff, M. C. (1981). Astrocytes, ependymal cells, and oligodendrocytes develop on schedule in dissociated cell cultures of embryonic rat brain. *Dev. Biol.* **83**, 301-310.

Akira, S., Nishio, Y., Inoue, M., Wang, X.-J., Wei, S., Matsusaka, T., Yoshida, K., Sudo, T., Naruto, M. and Kishimoto, T. (1994). Molecular cloning of APRF, a novel IFN-stimulated gene factor 3 p91-related transcription factor involved in the gp130-mediated signaling pathway. *Cell* **77**, 63-71.

Allan, E. H., Hilton, D. J., Brown, M. A., Evely, R. S., Yumita, S., Metcalf, D., Gough, N. M., Ng, K. W., Nicola, N. A. and Martin, T. J. (1990). Osteoblasts display receptors for and responses to leukemia-inhibitory factor. *J. Cell. Physiol.* **145**, 110-119.

Aloisi, F., Rosa, S., Testa, U., Bonsi, P., Russo, G., Peschle, C. and Levi, G. (1994). Regulation of leukemia inhibitory factor synthesis in cultured human astrocytes. *J. Immunol.* **152**, 5022-5031.

Bamber, B. A., Masters, B. A., Hoyle, G. W., Brinster, R. L. and Palmiter, R. D. (1994). Leukemia inhibitory factor induces neurotransmitter switching in transgenic mice. *Proc. Natl. Acad. Sci. USA* **91**, 7839-7843.

Banner, L. R. and Patterson, P. H. (1994). Major changes in the expression of the mRNAs for cholinergic differentiation factor/leukemia inhibitory factor and its receptor after injury to adult peripheral nerves and ganglia. *Proc. Natl. Acad. Sci. USA* **91**, 7109-7113.

Baron, R., Tross, R. and Vignery, A. (1984). Evidence of sequential remodeling in rat trabecular bone: morphology, dynamic histomorphometry, and changes during skeletal maturation. *Anat Rec* **208**, 137-145.

Bird, T. A., Sleath, P. R., deRoos, P. C., Dower, S. K. and Virca, G. D. (1991). Interleukin-1 represents a new modality for the activation of extracellular signal-regulated kinases/microtuble-associated protein-2 kinases. *J. Biol. Chem.* **266**, 22661-22670.

Bradley, A. (1987). Production and analysis of chimaeric mice. In *Teratocarcinomas and Embryonic Stem Cells: A Practical Approach* (ed. E. J. Robertson), pp. 113-151. Oxford: IRL Press.

Cheng, L., Gearing, D. P., White, L. S., Compton, D. L., Schooley, K. and Donovan, P. J. (1994). Role of leukemia inhibitory factor and its receptor in mouse primordial germ cell growth. *Development* **120**, 3145-3153.

Conquet, F. and Brulet, P. (1990). Developmental expression of myeloid leukemia inhibitory factor gene in preimplantation blastocysts and in extraembryonic tissue of mouse embryos. *Mol. Cell. Biol.* **10**, 3801-3805.

Curtis, R., Scherer, S. S., Somogyi, R., Adryan, K. M., Ip, N. Y., Zhu, Y., Lindsay, R. M. and Di Stefano, P. S. (1994). Retrograde axonal transport of LIF is increased by peripheral nerve injury: correlation with increased LIF expression in distal nerve. *Neuron* **12**, 191-204.

Davis, S., Aldrich, T. H., Stahl, N., Pan, L., Taga, T., Kishimoto, T., Ip, N. Y. and Yancopoulos, G. D. (1993). LIFRβ and gp130 as heterodimerizing signal transducers of the tripartite CNTF receptor. *Science* **260**, 1805-1808.

De Felici, M. and Dolci, S. (1991). Leukemia inhibitory factor sustains the survival of mouse primordial germ cells cultured on TM4 feeder layers. *Dev. Biol.* **147**, 281-284.

Dolci, S., Williams, D. E., Ernst, M. K., Resnick, J. L., Brannan, C. I., Lock, L. F., Lyman, S. D., Boswell, H. S. and Donovan, P. J. (1991). Requirement for mast cell growth factor for primordial germ cell survival in culture. *Nature* **352**, 809-811.

Donovan, P. J., Stott, D., Cairns, L. A., Heasman, J. and Wylie, C. C. (1986). Migratory and postmigratory mouse primordial germ cells behave differently in culture. *Cell* **44**, 831-838.

Escary, J. L., Perreau, J., Dumenil, D., Ezine, S. and Brulet, P. (1993). Leukaemia inhibitory factor is necessary for maintenance of haematopoietic stem cells and thymocyte stimulation. *Nature* **363**, 361-364.

Fan, G. and Katz, D. M. (1993). Non-neuronal cells inhibit catecholaminergic differentiation of primary sensory neurons: role of leukemia inhibitory factor. *Development* **118**, 83-93.

Ferrara, N., Winer, J. and Henzel, W. J. (1992). Pituitary follicular cells secrete an inhibitor of aortic endothelial cell growth: identification as leukemia inhibitory factor. *Proc. Natl. Acad. Sci. USA* **89**, 698-702.

Fletcher, F. A., Williams, D. E., Maliszewski, C., Anderson, D., Rives, M. and Belmont, J. W. (1990). Murine leukemia inhibitory factor enhances retroviral-vector infection efficiency of hematopoietic progenitors. *Blood* **76**, 1098-1103.

Fletcher, F. A., Moore, K. A., Ashkenazi, M., De Vries, P., Overbeek, P. A., Williams, D. E. and Belmont, J. W. (1991). Leukemia inhibitory factor improves survival of retroviral vector-infected hematopoietic stem cells in vitro, allowing efficient long-term expression of vector-encoded human adenosine deaminase in vivo. *J. Exp. Med.* **174**, 837-845.

Fukada, K. (1985). Purification and partial characterization of a cholinergic neuronal differentiation factor. *Proc. Natl. Acad. Sci. USA* **82**, 8795-8799.

Gearing, D. P., Thut, C. J., VandenBos, T., Gimpel, S. D., Delaney, P. B., King, J., Price, V., Cosman, D. and Beckmann, M. P. (1991). Leukemia inhibitory factor receptor is structurally related to the IL-6 signal transducer, gp130. *EMBO J.* **10**, 2839-2848.

Gearing, D. P. and Bruce, A. G. (1992). Oncostatin M binds the high-affinity leukemia inhibitory factor receptor. *New Biol.* **4**, 61-65.

Gearing, D. P., Comeau, M. R., Friend, D. J., Gimpel, S. D., Thut, C. J., McGourty, J., Brasher, K. K., King, J. A., Gillis, S., Mosley, B., Ziegler, S. F. and Cosman, D. (1992). The IL-6 signal transducer, gp130: An oncostatin M receptor and affinity converter for the LIF receptor. *Science* **255**, 1434-1437.

Gearing, D. P. (1993). The leukemia inhibitory factor and its receptor. *Adv. Immunol.* **53**, 31-58.

Gearing, D. P., Ziegler, S. F., Comeau, M. R., Friend, D., Thoma, B., Cosman, D., Park, L. and Mosley, B. (1994). Proliferative responses and binding properties of hematopoietic cells transfected with low-affinity receptors for leukemia inhibitory factor, oncostatin M, and ciliary neurotrophic factor. *Proc. Natl. Acad. Sci. USA* **91**, 1119-1123.

Gendron-Maguire, M., Mallo, M., Zhang, M. and Gridley, T. (1993). Hoxa-2 mutant mice exhibit homeotic transformation of skeletal elements derived from cranial neural crest. *Cell* **75**, 1317-1331.

Gillett, N. A., Lowe, D., Lu, L., Chan, C. and Ferrara, N. (1993). Leukemia inhibitory factor expression in human carotid plaques: possible mechanism for inhibition of large vessel endothelial regrowth. *Growth Factors* **9**, 301-305.

Godin, I., Deed, R., Cooke, J., Zsebo, K., Dexter, M. and Wylie, C. C. (1991). Effects of the *steel* gene product on mouse primordial germ cells in culture. *Nature* **352**, 807-809.

Gomperts, M., Garcia-Castro, M., Wylie, C. and Heasman, J. (1994). Interactions between primordial germ cells play a role in their migration in mouse embryos. *Development* **120**, 135-141.

Greenfield, E. M., Gornik, S. A., Horowitz, M. C., Donahue, H. J. and Shaw, S. M. (1993). Regulation of cytokine expression in osteoblasts by parathyroid hormone: rapid stimulation of interleukin-6 and leukemia inhibitory factor mRNA. *J. Bone Miner. Res.* **3**, 1163-1171.

Hendry, I. A., Murphy, M., Hilton, D. J., Nicola, N. A. and Bartlett, P. F. (1992). Binding and retrograde transport of leukemia inhibitory factor by the sensory nervous system. *J. Neurosci.* **12**, 3427-3434.

Hogan, B., Costantini, F. and Lacy, F. (1986). *Manipulating the Mouse Embryo.* Cold Spring Harbor:Cold Spring Harbor Laboratory.

Horowitz, M. C. (1993). Cytokines and estrogen in bone: Anti-osteoporotic effects. *Science* **260**, 626-627.

Ip, N. Y., Maisonpierre, P., Alderson, R., Friedman, B., Furth, M. E., Panayotatos, N., Squinto, S., Yancopoulos, G. D. and Lindsay, R. M. (1991). The neurotrophins and CNTF: specificity of action towards PNS and CNS neurons. *J. Physiol.* **85**, 123-130.

Ip, N. Y., Nye, S. H., Boulton, T. G., Davis, S., Taga, T., Li, Y., Birren, S. J., Yasukawa, K., Kishimoto, T., Anderson, D. J., Stahl, N. and Yancopoulos, G. D. (1992). CNTF and LIF act on neuronal cells via shared signaling pathways that involve the IL-6 signal transducing receptor component gp130. *Cell* **69**, 1121-1132.

Ip, N. Y. and Yancopoulos, G. D. (1992). Ciliary neurotrophic factor and its receptor complex. *Prog. Growth Factor Res.* **4**, 139-155.

Jilka, R. L., Hangoc, G., Girasole, G., Passeri, G., Williams, D. C., Abrams, J. S., Boyce, B., Broxmeyer, H. and Manolagas, S. C. (1992). Increased osteoclast development after estrogen loss: Mediation by interleukin-6. *Science* **257**, 88-91.

Kessler, J. A., Ludlam, W. H., Freidin, M. M., Hall, D. H., Michaelson, M. D., Spray, D. C., Dougherty, M. and Batter, D. K. (1993). Cytokine-induced programmed death of cultured sympathetic neurons. *Neuron* **11**, 1123-1132.

Kirby, M. L., Kumiski, D. H., Myers, T., Cerjan, C. and Mishima, N. (1993). Backtransplantation of chick cardiac neural crest cells cultured in LIF rescues heart development. *Dev Dyn* **198**, 296-311.

Kishimoto, T., Taga, T. and Akira, S. (1994). Cytokine signal transduction. *Cell* **76**, 253-262.

Kotzbauer, P. T., Lampe, P. A., Estus, S., Milbrandt, J. and Johnson, E. M., Jr. (1994). Postnatal development of survival responsiveness in rat sympathetic neurons to leukemia inhibitory factor and ciliary neurotrophic factor. *Neuron* **12**, 763-773.

Layton, M. J., Cross, B. A., Metcalf, D., Ward, L. D., Simpson, R. J. and Nicola, N. A. (1992). A major binding protein for leukemia inhibitory factor in normal mouse serum: identification as a soluble form of the cellular receptor. *Proc. Natl. Acad. Sci. USA* **89**, 8616-8620.

Leary, A. G., Wong, G. G., Clark, S. C., Smith, A. G. and Ogawa, M. (1990). Leukemia inhibitory factor differentiation-inhibiting activity/human interleukin for DA cells augments proliferation of human hematopoietic stem cells. *Blood* **75**, 1960-1964.

Lecron, J. C., Roblot, P., Chevalier, S., Morel, F., Alderman, E., Gombert, J. and Gascan, H. (1993). High circulating leukaemia inhibitory factor (LIF) in patients with giant cell arteritis: independent regulation of LIF and IL-6 under corticosteroid therapy. *Clin. Exp. Immunol.* **92**, 23-26.

Lorenzo, J. A., Sousa, S. L. and Leahy, C. L. (1990). Leukemia inhibitory factor (LIF) inhibits basal bone resorption in fetal rat long bone cultures. *Cytokine* **2**, 266-271.

Lütticken, C., Wegenka, U. M., Yuan, J., Buschmann, J., Schindler, C., Ziemiecki, A., Harpur, A. G., Wilks, A. F., Yasukawa, K., Taga, T., Kishimoto, T., Barbieri, G., Pellegrini, S., Sendtner, M., Heinrich, P. C. and Horn, F. (1994). Association of transcription factor APRF and protein

kinase Jak1 with the interleukin-6 signal transducer gp130. *Science* **263**, 89-92.

Lyman, S. D., James, L., VandenBos, T., de Vries, P., Brasel, K., Gliniak, B., Hollingsworth, L. T., Picha, K. S., McKenna, H. J., Splett, R. R., Fletcher, F. A., Maraskovsky, E., Farrah, T., Foxworthe, D., Williams, D. E. and Beckmann, M. P. (1993). Molecular cloning of a ligand for the flt3/flk-2 tyrosine kinase receptor: A proliferative factor for primitive hematopoietic cells. *Cell* **75**, 1157-1167.

Martin, T. J., Allan, E. H., Evely, R. S. and Reid, I. R. (1992). Leukemia inhibitory factor and bone cell function. In *Polyfunctional Cytokines: IL-6 and LIF (CIBA Found. Symp. No. 167)* (ed. G. R. Bock, J. Marsh and K. Widdows), pp. 141-155. Chichester: Wiley.

Martinou, J. C., Martinou, I. and Kato, A. C. (1992). Cholinergic differentiation factor (CDF/LIF) promotes survival of isolated rat embryonic motoneurons in vitro. *Neuron* **8**, 737-744.

Masu, Y., Wolf, E., Holtmann, B., Sendtner, M., Brem, G. and Thoenen, H. (1993). Disruption of the CNTF gene results in motor neuron degeneration. *Nature* **365**, 27-32.

Matsui, Y., Toksoz, D., Nishikawa, S., Nishikawa, S., Williams, D., Zsebo, K. and Hogan, B. L. (1991). Effect of Steel factor and leukaemia inhibitory factor on murine primordial germ cells in culture. *Nature* **353**, 750-752.

Mayer, M., Bhakoo, K. and Noble, M. (1994). Ciliary neurotrophic factor and leukemia inhibitory factor promote the generation, maturation and survival of oligodendrocytes in vitro. *Development* **120**, 143-153.

Metcalf, D., Hilton, D. J. and Nicola, N. A. (1988). Clonal analysis of the actions of the murine leukemia inhibitory factor on leukemic and normal murine hemopoietic cells. *Leukemia* **2**, 216-221.

Metcalf, D. and Gearing, D. P. (1989a). Fatal syndrome in mice engrafted with cells producing high levels of the leukemia inhibitory factor. *Proc. Natl. Acad. Sci. USA* **86**, 5948-5952.

Metcalf, D. and Gearing, D. P. (1989b). A myelosclerotic syndrome in mice engrafted with cells producing high levels of leukemia inhibitory factor (LIF). *Leukemia* **3**, 847-852.

Metcalf, D., Nicola, N. A. and Gearing, D. P. (1990). Effects of injected leukemia inhibitory factor on hematopoietic and other tissues in mice. *Blood* **76**, 50-56.

Metcalf, D., Waring, P. and Nicola, N. A. (1992). Actions of leukemia inhibitory factor on megakaryocyte and platelet formation. In *Polyfunctional Cytokines: IL-6 and LIF (CIBA Found. Symp. No. 167)* (ed. G. R. Bock, J. Marsh and K. Widdows), pp. 174-182. Chichester: Wiley.

Moran, C. S., Campbell, J. H., Simmons, D. L. and Campbell, G. R. (1994). Human leukemia inhibitory factor inhibits development of experimental atherosclerosis. *Arterioscler. Thromb.* **14**, 1356-1363.

Mori, M., Yamaguchi, K. and Abe, K. (1989). Purification of a lipoprotein lipase-inhibiting protein produced by a melanoma cell line associated with cancer cachexia. *Biochem. Biophys. Res. Commun.* **160**, 1085-1092.

Mortensen, R. M., Conner, D. A., Chao, S., Geisterfer-Lowrance, A. A. and Seidman, J. G. (1992). Production of homozygous mutant ES cells with a single targeting construct. *Mol. Cell. Biol.* **12**, 2391-2395.

Murphy, M., Reid, K., Hilton, D. J. and Bartlett, P. F. (1991). Generation of sensory neurons is stimulated by leukemia inhibitory factor. *Proc. Natl. Acad. Sci. USA* **88**, 3498-3501.

Murphy, M., Reid, K., Brown, M. A. and Bartlett, P. F. (1993). Involvement of leukemia inhibitory factor and nerve growth factor in the development of dorsal root ganglion neurons. *Development* **117**, 1173-1182.

Murray, R., Lee, F. and Chiu, C. P. (1990). The genes for leukemia inhibitory factor and interleukin-6 are expressed in mouse blastocysts prior to the onset of hemopoiesis. *Mol. Cell. Biol.* **10**, 4953-4956.

Nawa, H. and Patterson, P. H. (1990). Separation and partial characterization of neuropeptide-inducing factors in heart cell conditioned medium. *Neuron* **4**, 269-277.

Nishiyama, K., Collodi, P. and Barnes, D. (1993). Regulation of glial fibrillary acidic protein in serum-free mouse embryo (SFME) cells by leukemia inhibitory factor and related peptides. *Neurosci. Lett.* **163**, 114-116.

Parfitt, A. M., Drezner, M. K., Glorieux, F. H., Kanis, J. A., Malluche, H., Meunier, P. J., Ott, S. M. and Recker, R. R. (1987). Bone histomorphometry: standardization of nomenclature, symbols, and units. Report of the ASBMR Histomorphometry Nomenclature Committee. *J. Bone Miner. Res.* **2**, 595-610.

Pesce, M., Farrace, M. G., Piacentini, M., Dolci, S. and De Felici, M. (1993). Stem cell factor and leukemia inhibitory factor promote primordial germ cell survival by suppressing programmed cell death (apoptosis). *Development* **118**, 1089-1094.

Poli, V., Balena, R., Fattori, E., Markatos, A., Yamamoto, M., Tanaka, H., Ciliberto, G., Rodan, G. A. and Costantini, F. (1994). Interleukin-6 deficient mice are protected from bone loss caused by estrogen depletion. *EMBO J.* **13**, 1189-1196.

Rao, M. S., Tyrrell, S., Landis, S. C. and Patterson, P. H. (1992). Effects of ciliary neurotrophic factor (CNTF) and depolarization on neuropeptide expression in cultured sympathetic neurons. *Dev. Biol.* **150**, 281-293.

Rao, M. S., Sun, Y., Escary, J. L., Perreau, J., Tresser, S., Patterson, P. H., Zigmond, R. E., Brulet, P. and Landis, S. C. (1993). Leukemia inhibitory factor mediates an injury response but not a target-directed developmental transmitter switch in sympathetic neurons. *Neuron* **11**, 1175-1185.

Reid, I. R., Lowe, C., Cornish, J., Skinner, S. J. M., Hilton, D. J., Willson, T. A., Gearing, D. P. and Martin, T. J. (1990). Leukemia inhibitory factor: a novel bone-active cytokine. *Endocrinology* **126**, 1416-1420.

Resnick, J. L., Bixler, L. S., Cheng, L. and Donovan, P. J. (1992). Long-term proliferation of mouse primordial germ cells in culture. *Nature* **359**, 550-551.

Smith, A. G., Heath, J. K., Donaldson, D. D., Wong, G. G., Moreau, J., Stahl, M. and Rogers, D. (1988). Inhibition of pluripotential embryonic stem cell differentiation by purified polypeptides. *Nature* **336**, 688-690.

Smith, E. P., Boyd, J., Frank, G. R., Takahashi, H., Cohen, R. M., Specker, B., Williams, T. C., Lubahn, D. B. and Korach, K. S. (1994). Estrogen resistance by a mutation in the estrogen-receptor gene in a man. *N. Engl. J. Med.* **331**, 1056-1089.

Soriano, P., Montgomery, C., Geske, R. and Bradley, A. (1991). Targeted disruption of the c-src proto-oncogene leads to osteopetrosis in mice. *Cell* **64**, 693-702.

Stewart, C. L., Kaspar, P., Brunet, L. J., Bhatt, H., Gadi, I., Kontgen, F. and Abbondanzo, S. J. (1992). Blastocyst implantation depends on maternal expression of leukaemia inhibitory factor. *Nature* **359**, 76-79.

Takahashi, R., Yokoji, H., Misawa, H., Hayashi, M., Hu, J. and Deguchi, T. (1994). A null mutation in the human CNTF gene is not causally related to neurological diseases. *Nat. Genet.* **7**, 79-84.

Thaler, C. D., Suhr, L., Ip, N. and Katz, D. M. (1994). Leukemia inhibitory factor and neurotrophins support overlapping populations of rat nodose sensory neurons in culture. *Dev. Biol.* **161**, 338-344.

Thoma, B., Bird, T. A., Friend, D. J., Gearing, D. P. and Dower, S. K. (1994). Oncostatin M and leukemia inhibitory factor trigger overlapping and different signals through partially shared receptor complexes. *J. Biol. Chem.* **269**, 6215-6222.

Thomson, B. M., Saklatvala, J. and Chambers, T. J. (1986). Osteoblasts mediate interleukin 1 stimulation of bone resorption by rat osteoclasts. *J. Exp. Med.* **164**, 104-112.

Till, J. E. and McCulloch, E. A. (1961). A direct measurement of the radiation sensitivity of normal mouse bone marrow cells. *Radiat. Res.* **14**, 213.

Tomida, M., Yamamoto-Yamaguchi, Y. and Hozumi, M. (1984). Purification of a factor inducing differentiation of mouse myeloid leukemic M1 cells from conditioned medium of mouse fibroblast L929 cells. *J. Biol. Chem.* **259**, 10978-10982.

Tsarfaty, I., Resau, J. H., Rulong, S., Keydar, I., Faletto, D. L. and Vande Woude, G. F. (1992). The met proto-oncogene receptor and lumen formation. *Science* **257**, 1258-1261.

Tsarfaty, I., Rong, S., Resau, J. H., Rulong, S., da Silva, P. P. and Vande Woude, G. F. (1994). The Met proto-oncogene mesenchymal to epithelial cell conversion. *Science* **263**, 98-101.

Ure, D. R. and Campenot, R. B. (1994). Leukemia inhibitory factor and nerve growth factor are retrogradely transported and processed by cultured rat sympathetic neurons. *Dev. Biol.* **162**, 339-347.

Van Beek, E., Van Der Wee-Pals, L., Van De Ruit, M., Nijweide, P., Papapoulos, S. and Löwik, C. (1993). Leukemia inhibitory factor inhibits osteoclastic resorption, growth, mineralization, and alkaline phosphatase activity in fetal mouse metacarpal bones in culture. *J. Bone Miner. Res.* **8**, 191-198.

Verfaillie, C. and McGlave, P. (1991). Leukemia inhibitory factor/human interleukin for DA cells: a growth factor that stimulates the in vitro development of multipotential human hematopoietic progenitors. *Blood* **77**, 263-270.

Whitlock, C. A. and Witte, O. N. (1982). Long-term culture of B lymphocytes and their precursors from murine bone marrow. *Proc. Natl. Acad. Sci. USA* **79**, 3608-3612.

Williams, R. L., Hilton, D. J., Pease, S., Willson, T. A., Stewart, C. L., Gearing, D. P., Wagner, E. F., Metcalf, D., Nicola, N. A. and Gough, N. M. (1988). Myeloid leukaemia inhibitory factor maintains the developmental potential of embryonic stem cells. *Nature* **336**, 684-687.

Wolf, E., Kramer, R., Polejaeva, I., Thoenen, H. and Brem, G. (1994). Efficient generation of chimaeric mice using embryonic stem cells after long-

term culture in the presence of ciliary neurotrophic factor. *Transgenic Res* **3**, 152-158.

Yamamori, T., Fukada, K., Aebersold, R., Korsching, S., Fann, M. J. and Patterson, P. H. (1989). The cholinergic neuronal differentiation factor from heart cells is identical to leukemia inhibitory factor. *Science* **246**, 1412-1416.

Yoshida, K., Chambers, I., Nichols, J., Smith, A., Saito, M., Yasukawa, K., Shoyab, M., Taga, T. and Kishimoto, T. (1994). Maintenance of the pluripotential phenotype of embryonic stem cells through direct activation of gp130 signaling pathways. *Mech. Dev.* **45**, 163-171.

(Accepted 8 February 1995)